Research Square

Preprints are preliminary reports that have not undergone peer review.
They should not be considered conclusive, used to inform clinical practice,
or referenced by the media as validated information.

Characterization of the Moreras Fault Zone and related faults (Águilas Arc, Eastern Betic Cordillera)

Iván Medina-Cascales

ivan.medina@ua.es

Universidad de Alicante

Iván Martin-Rojas

Universidad de Alicante

Francisco J. García-Tortosa

Universidad de Jaén

Antonio Borrego

Pedro Alfaro

Universidad de Alicante

Research Article

Keywords:

Posted Date: October 6th, 2026

DOI: https://doi.org/10.21203/rs.3.rs-10230556/v1

License: This work is licensed under a Creative Commons Attribution 4.0 International License.
Read Full License

Additional Declarations: No competing interests reported.

Characterization of the Moreras Fault Zone and related faults (Águilas Arc, Eastern Betic Cordillera)

Iván Medina-Cascales[1], Iván Martin-Rojas[1], Francisco J. García-Tortosa[2], Antonio Borrego, Pedro Alfaro[1]

1 Departamento de Ciencias de la Tierra y del Medio Ambiente, Universidad de Alicante, 03690, San Vicente del Raspeig, Alicante, Spain; ivan.medina@ua.es , ivan.martin@ua.es , pedro.alfaro@ua.es

2 Departamento de Geología, Universidad de Jaén, Campus Las Lagunillas, 23071, Jaén, Spain; gtortosa@ujaen.es

ORCID IDs: Iván Medina-Cascales: 0000-0002-9287-2425; Iván Martin-Rojas: 0000-0002-9109-0384; Francisco J. García-Tortosa: 0000-0003-3681-5829; Pedro Alfaro: 0000-0002-2753-2969

Corresponding author: Iván Medina Cascales, ivan.medina@ua.es

Abstract

The Moreras Fault Zone (MFZ) is a major structure that accommodated deformation in the Águilas Arc (Eastern Betic Cordillera, SE Spain) during the Miocene. This and other faults within the arc have not been subjected to detailed tectonic studies, leaving several unresolved questions regarding their structure and activity. This study presents a new structural characterization of the MFZ and adjacent faults based on detailed geological mapping, structural data, and observations of Neogene-Quaternary deformation. The MFZ is a ca. 23 km-long, 2.8 km-wide fault zone formed by two major N105E strands and numerous secondary faults. It behaved as an oblique structure, accommodating approximately 10 km of right-lateral displacement. The mapping clarifies the relationships between the MFZ and neighbouring structures, including the N060E Almenara Fault Zone and Peñas Blancas fault system and the N90E Cape Tiñoso fault system. Contrary to previous interpretations, the MFZ is a distinct structure from the Cape Tiñoso fault system and the offshore Mazarrón Escarpment faults. Instead, it terminates against the left-lateral Peñas Blancas fault system, which offsets and disrupts its eastern continuation. Evidence for Neogene-Quaternary deformation indicates significant Miocene tectonic activity in all faults, whereas Quaternary deformation is scarce and restricted to subtle features in alluvial deposits along limited fault segments. Together with low regional seismicity and geodetic slip rates, this suggests a marked decrease in tectonic activity since the Pliocene, supporting a progressive northward migration of deformation within the Internal Zone of the Eastern Betic Cordillera, from the Águilas Arc toward the Eastern Betic Shear Zone.

1. Introduction

In the Eastern Betic Cordillera (SE Spain), the current NNW-SSE oblique convergence between the Nubia and Eurasian plates produces crustal shortening (e.g., Buforn *et al*., 2004; Serpelloni *et al*., 2007; Pérez-Peña *et al*., 2010; Vernant *et al*., 2010; Koulali *et al*., 2011; Spakman *et al*., 2018), which is accommodated in a wide deformation zone. In this context, the presence of an indenter in the Mediterranean Sea (Coppier *et al*., 1989; Palano *et al*., 2015; Borque *et al*., 2019) has resulted in a SW-NE to W-E oriented tectonic arc (Fig. 1).

The outer part of this arc is a tectonic corridor known as the Eastern Betic Shear Zone (EBSZ) (Bousquet, 1979; Montenat *et al*., 1987; De Larouziere *et al*., 1988; Silva *et al.*, 1993) (Fig. 1). The EBSZ is formed by a series of left-lateral and reverse faults that have been widely studied from a structural, tectonic, palaeoseismological, seismological, and geodetic approach (e.g., Bousquet, 1979; Booth-Rea *et al*., 2003; Masana *et al*., 2004; Gràcia *et al*., 2006; Alfaro *et al*., 2012; Martínez-Díaz *et al*., 2012; Buontempo and Wuestefeld, 2013; Martín-Banda *et al*., 2016; Martin-Rojas *et al*., 2015). The shortening absorbed by the faults within the EBSZ ranges between 1.5 ± 0.3 mm/yr and in 0.7 ± 0.2 mm/yr (Echeverria *et al*., 2013 and 2015; Borque *et al.*, 2019). Some of these structures were the seismogenic sources of destructive earthquakes in SE Spain, such as the 1829 Torrevieja earthquake (IMSK = IX–X; Ms = 6.3–6.9, Muñoz and Udías, 1991), the 1919 Jacarilla-Torremendo earthquake (mb = 5.1 and 5.2) (Batlló *et al.*, 2015), and the 2011 Lorca earthquake (M = 5.2) (Martínez-Díaz *et al*., 2012).

South of the EBSZ, the inner part of the tectonic arc corresponds to a highly folded and faulted region known as the Águilas Arc (Coppier *et al*., 1989) (Fig. 1). The Águilas Arc is structured mainly by WNW-ESE to W-E right-lateral faults and NE-SW left-lateral faults (Ott d'Estevou and Montenat, 1985; De Larouzière *et al*., 1987; Coppier *et al*., 1989). These structures have accommodated deformation through different deformational stages from the middle Miocene to the Quaternary (Ott d'Estevou and Montenat, 1985; Coppier *et al*., 1989). However, in contrast to the EBSZ, the faults of the Águilas Arc host a lower number of structural and tectonic studies. Most of these faults were firstly defined during the last decades of the 20th century by studies focused on the tectono-sedimentary processes that conformed the Neogene-Quaternary basins in the Eastern Betic Cordillera, especially during the Miocene (Ott d'Estevou and Montenat, 1985; Ott d'Estevou *et al*., 1988; De Larouzière *et al*., 1987 and 1988; Coppier *et al*., 1989 and 1990; De Larouzière and Ott d'Estevou, 1990; Montenat *et al*., 1990; Montenat and Ott d'Estevou, 1992 and 1999). These pioneer works provided the first regional tectonic maps of the Águilas Arc and pointed the neotectonic activity of some of the main faults. However, these were regional studies that were not focused on characterizing these faults in detail.

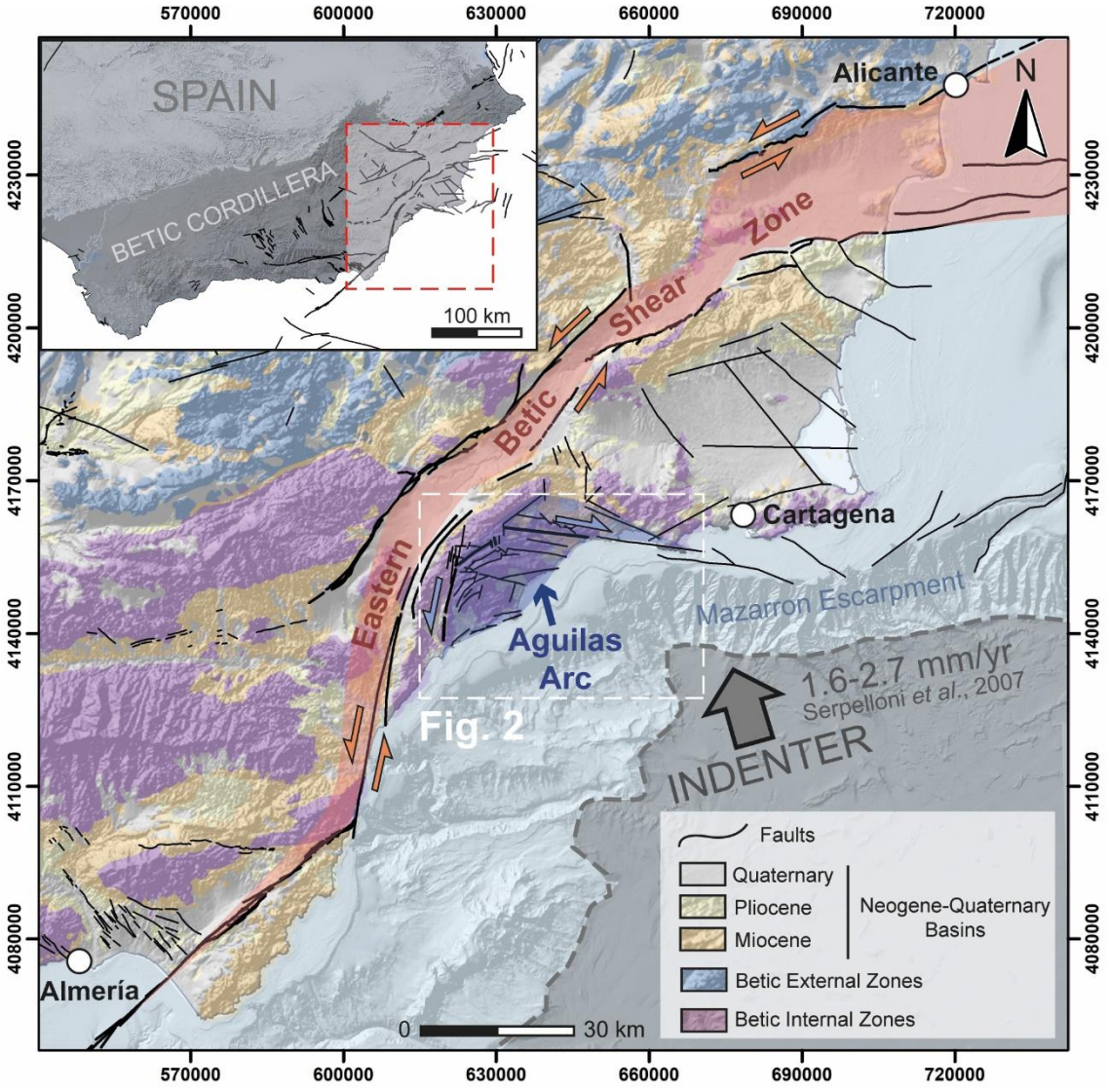


Fig. 1 Geological map of the Eastern Betic Cordillera depicting the main tectonic features accommodating NNW-SSE shortening in the Betic Internal Zone. The presence of an indenter in the Mediterranean Sea resulted in the Eastern Betics Tectonic Arc, formed by the EBSZ to the north and the Águilas Arc to the south. Fault traces after Coppier *et al*. (1989) and the QAFI database (García-Mayordomo *et al*., 2012). DEM source: Centro Nacional de Información Geográfica (CNIG, https://centrodedescargas.cnig.es/CentroDescargas/index.jsp. Bathymetry source: Instituto Hidrográfico de la Marina (IHM, https://cdihm.cnig.es/CentroDescargasIHM/home)

Moreover, knowledge about the Quaternary activity in the Águilas Arc remains limited in comparison to the EBSZ. On the one hand, the seismicity in this region is very low. The number of recorded events is very reduced in comparison to the EBSZ. The two main recorded historic earthquakes (AD 1596 and AD 1882) show maximum intensities of IV-V. The most remarkable activity during the instrumental period corresponds to the 1996 Mazarrón seismic series, with a main event of magnitude 4.5 and an intensity of V (Baena *et al*., 1993; Martinez-Solares and Mezcua, 2002; García-Mayordomo, 2005; IGN, *n.d.*). On the other hand, research focused directly on active tectonics is very scarce in the region. Evidence of potential quaternary activity along faults have been suggested mostly from geomorphological studies that examined the tectonic influence on the formation and evolution of alluvial fan systems, marine platforms, and drainage networks during the Quaternary (Bardají *et al*., 1990 and 2015; Silva *et al*., 1993; Bardají, 1999; Zazo *et al*., 2003). The results of these studies were used to include some of the

major structures of the Águilas Arc as neotectonic and/or active faults in maps and databases (ITGE, 1993; Baena-Pérez *et al.,* 1998; García-Tortosa *et al*., 2004a, 2004b, 2004c, and 2004d; Booth-Rea *et al*., 2009; García-Mayordomo *et al*., 2012; García-Mayordomo and Martín-Banda, 2022).

One of the main structures in the Águilas Arc is the Moreras Fault. This fault has been described by previous authors as a major right-lateral fault that has accommodated deformation during the Neogene (e.g., De Larouziere *et al*., 1987; Coppier *et al*., 1989). The total length of this fault has been revised over the years. In the present day, the fault is considered as part of a larger structure together with other offshore faults that affect the Mazarrón Escarpment, the continental slope in this region (Coppier *et al*., 1989; ITGE, 1990; Díaz, del Río *et al*., 1991; Acosta *et al*., 2013; García-Mayordomo *et al*., 2012; García-Mayordomo and Martín-Banda, 2022). Moreover, although the Moreras Fault is classified as active during the Quaternary based mainly on geomorphological criteria (Bardají, 1999; García-Tortosa and Leyva 2004a) its activity during the Upper Pleistocene-Holocene is not demonstrated yet (García-Mayordomo *et al*., 2012; García-Mayordomo and Martín-Banda, 2022).

This work presents the results of field-based research focused on the Moreras Fault −from now referred to as the Moreras Fault Zone (MFZ)− and adjacent faults, located in the northern sector of the Águilas Arc (Fig. 2). The main aim of this study is to provide an updated characterization of these faults, including new fault data, such as detailed geometries of their traces and surface structural data. Additionally, tectonic deformation features are described in the Neogene-Quaternary deposits along the faults, focusing on geological evidence of Quaternary deformation. With this data, the MFZ is brought under discussion in terms of fault length, segmentation, and Quaternary activity.

2. Geological setting

The Águilas Arc (Fig. 2) was formed as part of the Betic Cordillera, when the Alboran plate (Andrieux *et al*.,1971) collided against the southern palaeomargin of Iberia during the early to middle Miocene (Tapponnier, 1977; Durand-Delga and Fontbote, 1980; Sanz de Galdeano, 1983; Martin-Algarra, 1987). This collision established two important domains in the Betic Cordillera: the Internal Zone, formed by the Palaeozoic and Mesozoic metamorphic rocks of the Alboran plate, and the Betic External Zone, formed by the Mesozoic to Paleogene sedimentary rocks of the Iberian palaeomargin (Fallot, 1948; Azéma *et al*., 1979). During the Miocene, these geological domains have been subjected to several deformational stages involving shortening and stretching (Sanz de Galdeano, 1990; García-Dueñas *et al*., 1992; Galindo-Zaldívar *et al.*, 1993; Duggen *et al*., 2005; Giaconia *et al*., 2014; Gómez de la Peña *et al.,* 2021).

The geodynamic setting that defines the current tectonics in the Betic Cordillera was established in the late Tortonian. This setting is conditioned by the NNW-SSE oblique convergence between the Nubia and Eurasian plates (approximately 5-6 mm/yr, e.g., Stich *et al*., 2006; Serpelloni *et al*., 2007; DeMets *et al*., 2010; Nocquet, 2012). The way the deformation is accommodated in the Eastern Betic Cordillera is conditioned by the presence of a thin and rigid block of oceanic crust located below the Alboran Sea, the western branch of the Algero-Balearic Basin. This block acted as a tectonic indenter, transferring a fraction of the plate convergence to the north and producing NNW-SSE to N-S shortening in the Eastern Betic Cordillera (Coppier *et al*., 1989; Palano *et al*., 2015; Borque *et al*., 2019; Madarieta-Txurruka *et al.*, 2025).

Shortening in the Betic Cordillera intensely deformed the External and Internal zones. In the External Zone, the Cazorla-Alcaraz-Hellín tectonic arc was developed (Álvaro *et al*., 1975; Rodríguez-Estrella, 1979; Mandeville, 1993; Andrieux y Nebbad, 1996; Platt *et al*., 2003; Pérez-Valera *et al*., 2017 and 2022; Trigueros-Ramos *et al*., 2024), while in the Internal Zone, the Eastern Betics Tectonic Arc was formed. The Eastern Betics Tectonic Arc, which consists of the EBSZ to the north and the Águilas Arc in its core to the south.

In the Aguilas Arc, deformation of the Betic Internal Zone gave rise to large SW-NE to W-E folds, such as the Las Moreras, Lomo de Bas, Almenara, or the Algarrobo anticlines (Fig. 2). Moreover, a series of strike-slip faults formed to accommodate deformation within the arc, such as the NE-SW left-lateral Terreros and Almenara faults, or the WNW-ESE to W-E right-lateral Moreras Fault Zone and Lomo de Bas Fault (Montenat *et al*., 1987; De Larouzière *et al*., 1987 and 1988; Montenat and Ott d'Estevou, 1988; Álvarez-Lobato, 1987; Coppier *et al*., 1989; Silva *et al.*, 1993; Booth-Rea *et al*., 2004; Bardají *et al*., 2010 and 2015; Medina-Cascales *et al.*, in press) (Fig. 2). The Moreras Fault Zone has been documented as one of the main structures in the Águilas Arc accommodating deformation during the Neogene. The onshore expression of this structure is described as two N100E right-lateral faults, both thrusting north, that extends ca. 40 km bounding the Las Moreras anticline to the north and south (De Larouzière *et al*., 1987; Coppier *et al*., 1989; Silva *et al.*, 1993). Adittionally, some authors indicate that the Moreras Fault Zone may present one or several offshore segments that extends to the SE along the continental shelf (Coppier *et al.*, 1989; ITGE, 1990; Díaz del Río, 1991; Acosta *et al.*, 2013) (Fig. 2).

Folding and faulting during the Miocene led to the individualization of sedimentary basins within the Águilas Arc, such as the Ramonete, Águilas-Terreros, and Cope basins (Fig. 2) (Montenat, 1977; Montenat *et al*., 1987; Montenat and Ott d'Estevou, 1988; De Larouzière *et al*., 1987; Ott d'Estevou *et al*., 1988; Coppier *et al*., 1989; De Larouzière and Ott d'Estevou, 1990; Montenat and Serrano, 1995). Moreover, during the late Tortonian, the northern sector of the arc was subjected to local extension, resulting in the opening of the Mazarrón sedimentary basin (De Larouzière *et al*., 1987; Coppier *et al.*, 1989; Duggen *et al*., 2005).

The Neogene-Quaternary basins in the study area (Fig. 3) are the Mazarrón, Ramonete, and Bolnuevo basins. The basement of these basins is formed by the metamorphic rocks of the Betic Internal Zone, specifically by the Nevado-Filábride and the Alpujárride complexes (Fig. 3) (Egeler and Simon, 1969; Puga *et al*., 1974; Sanz de Galdeano, 1997; Kozur *et al*., 1985; García-Tortosa *et al*., 2000; García-Tortosa, 2002). These rocks crop out in the basin margins and in the main structural reliefs. Unconformably over the basement lies the sedimentary infill of the basins, consisting of Miocene to Quaternary deposits (Fig. 3) (Montenat, 1973; De Larouziére, 1985; Griveaud, 1989; Bardají, 1999; Ortiz *et al*., 2020; Torres *et al*., 2020). The older infilling is found in the Ramonete and Bolnuevo basins, consisting of Burdigalian to Lower Tortonian detritic, fan-delta deposits (Griveaud, 1989). The late Tortonian is represented in all the basins by pelagic marls and turbiditic deposits (De Larouzière et al., 1987; De Larouzière and Ott d'Estevou, 1990). Moreover, during this time, the opening of the Mazarrón Basin provoked an anatectic volcanic episode, resulting in the extrusion of large volumes of andesitic and rhyolitic volcanic rocks (Fig. 3) (Bellon *et al*., 1983; Bolze and Ott d'Estevou, 1986; Hernández *et al*., 1987; De Larouziére and Ott d'Estevou, 1990; Duggen *et al*., 2005; Rodrigo-Naharro *et al*., 2013 and 2018). Unconformably over the late Tortonian lie Messinian marine deposits (De Larouzière *et al*., 1987; De Larouzière and Ott d'Estevou, 1990). The lower Pliocene is underrepresented in the study area and consists of shallow marine rocks cropping out close to the coastline in the Ramonete and Bolnuevo basins, and in the northernmost margin of the Mazarrón Basin (Montenat, 1975;

De Larouziere *et al.* 1987; De Larouzière and Ott d'Estevou, 1990; Leyva-Cabello *et al.*, 2010). The continentalization of the basins took place during the Pliocene (De Larouziere *et al*. 1987; De Larouzière and Ott d'Estevou, 1990; Leyva-Cabello *et al.*, 2010). In the Quaternary, restricted sedimentation in these basins formed several generations of alluvial fan systems, as well as fluvial and marine terraces (Bardají, 1999; Zazo *et al*., 2003; García-Tortosa and Leyva, 2004a).

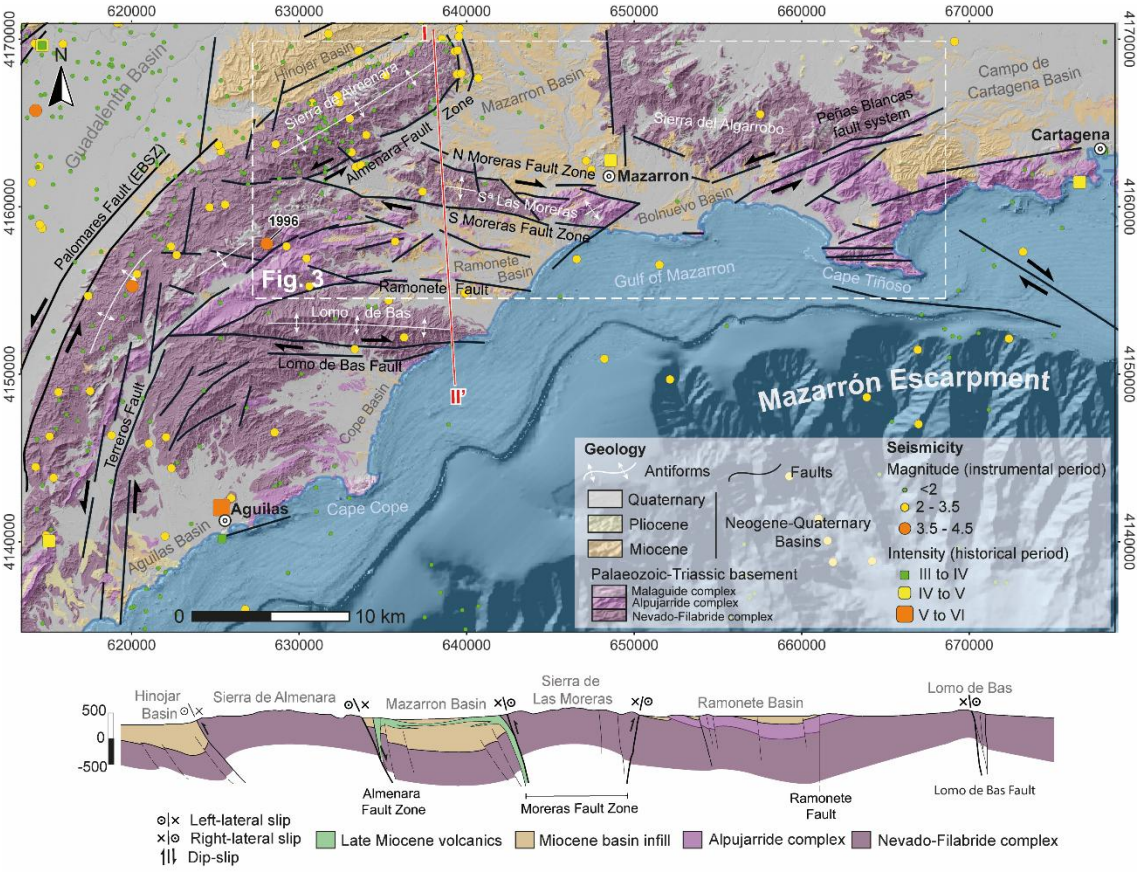


Fig. 2 Simplified geological map and geological cross-section (II-II') of the Águilas Arc showing the main tectonic structures. The white dashed frame marks the extension of the study area in figure 3. Fault traces after Coppier *et al*. (1989), Acosta *et al*. (2013) and this work

3. Characterization of the Moreras Fault Zone and related faults

Faults in the study area (Fig. 3) have been defined through a detailed geological mapping, combining field observations and interpretation of high resolution orthorectified aerial photographs and digital elevation models (DEMs) with a resolution of 2 m per pixel (Centro Nacional de Información Geográfica, https://centrodedescargas.cnig.es). The result is a map including the onshore extension of the fault traces, as well as the basement and Neogene-Quaternary basin infill deposits that crop out along the region (Fig. 3). Additionally, fault structural and kinematic data, including slip surface orientations and slickenlines, have been collected to complement the fault characterization. In this section, these geometric and structural features are described in detail for the Moreras Fault Zone (MFZ) and geometrically related structures, such as the Almenara Fault Zone and the Peñas Blancas and Cape Tiñoso fault systems (Figs. 3 to 5).

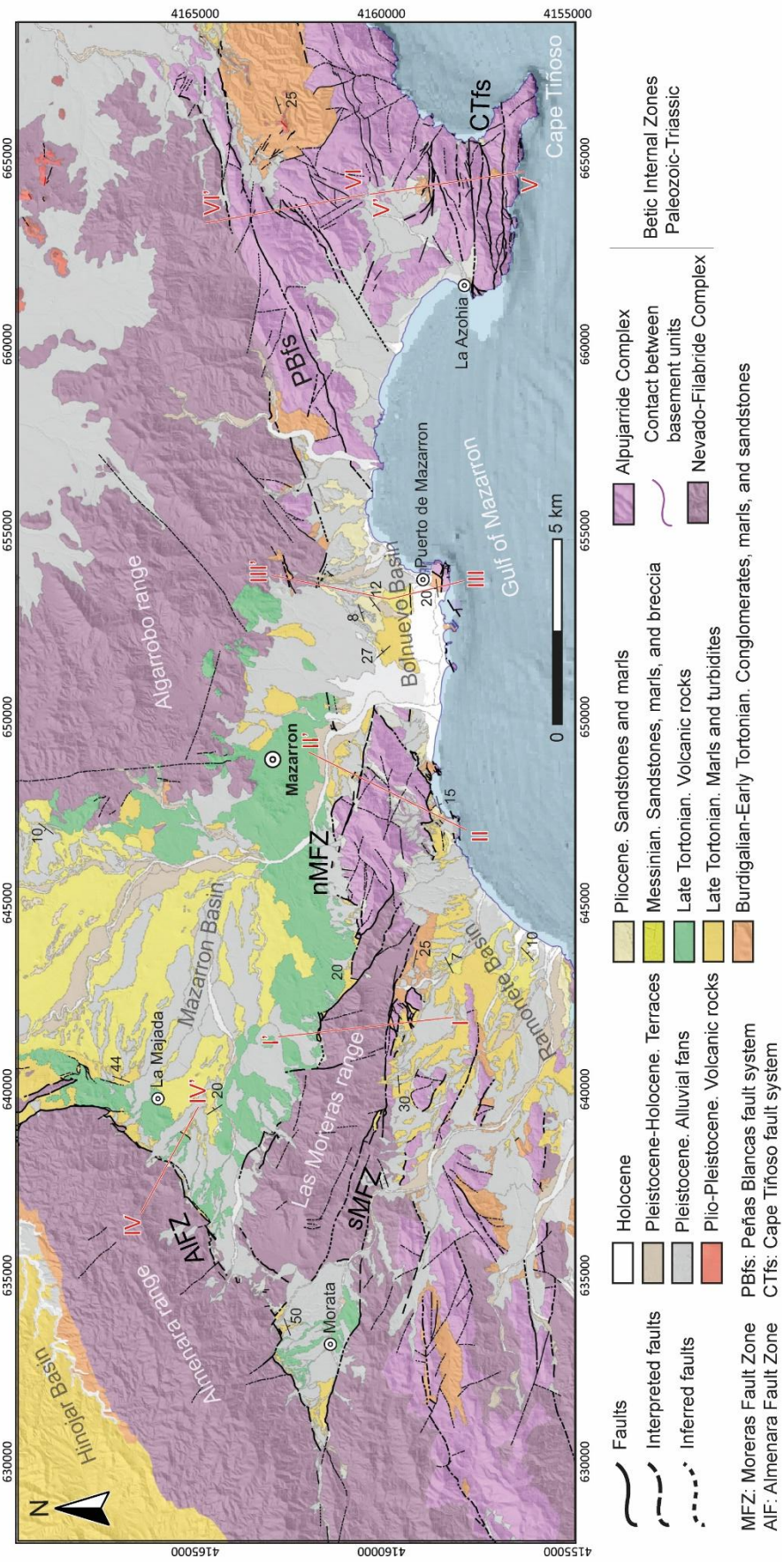


Fig. 3 Geological map of the study area, displaying the Moreras Fault Zone (MFZ) and neighboring faults characterized in this work. Red lines mark the position of cross-sections in figure 4

3.1. The Moreras Fault Zone

The Moreras Fault Zone (henceforth referred to as MFZ) extends approximately 21 km with a mean N105E direction (Fig. 3). The main landscape feature related to the fault zone are the uplifted reliefs of the ca. N100E Las Moreras anticline (Corbella Marti, 1969), which are formed by rocks of the Nevado-Filábride complex to the west superposed by tectonic units of the Alpujárride complex to the east (García-Tortosa, 2002) (Figs. 3 and 4). The surface structure of the MFZ consists of a ca. 2.8 km-wide fault zone formed by two main, roughly subparallel fault strands. From now, they are referred as the southern and northern MFZ, respectively. These strands bound and offset the Las Moreras anticline to the north and to the south. Apart from the two main strands, the MFZ is formed by a high number of secondary faults with variable orientation. The most remarkable of these secondary structures is a ca. 5 km-long fault, striking ca. N125E, that crosses and offsets the entire anticline. This structure separates the MFZ into a western and an eastern sector (Fig. 3). The complex array of main and secondary faults forming the MFZ internally deforms the Las Moreras anticline, giving a right-lateral, duplex-like structure in map view (Fig.3).

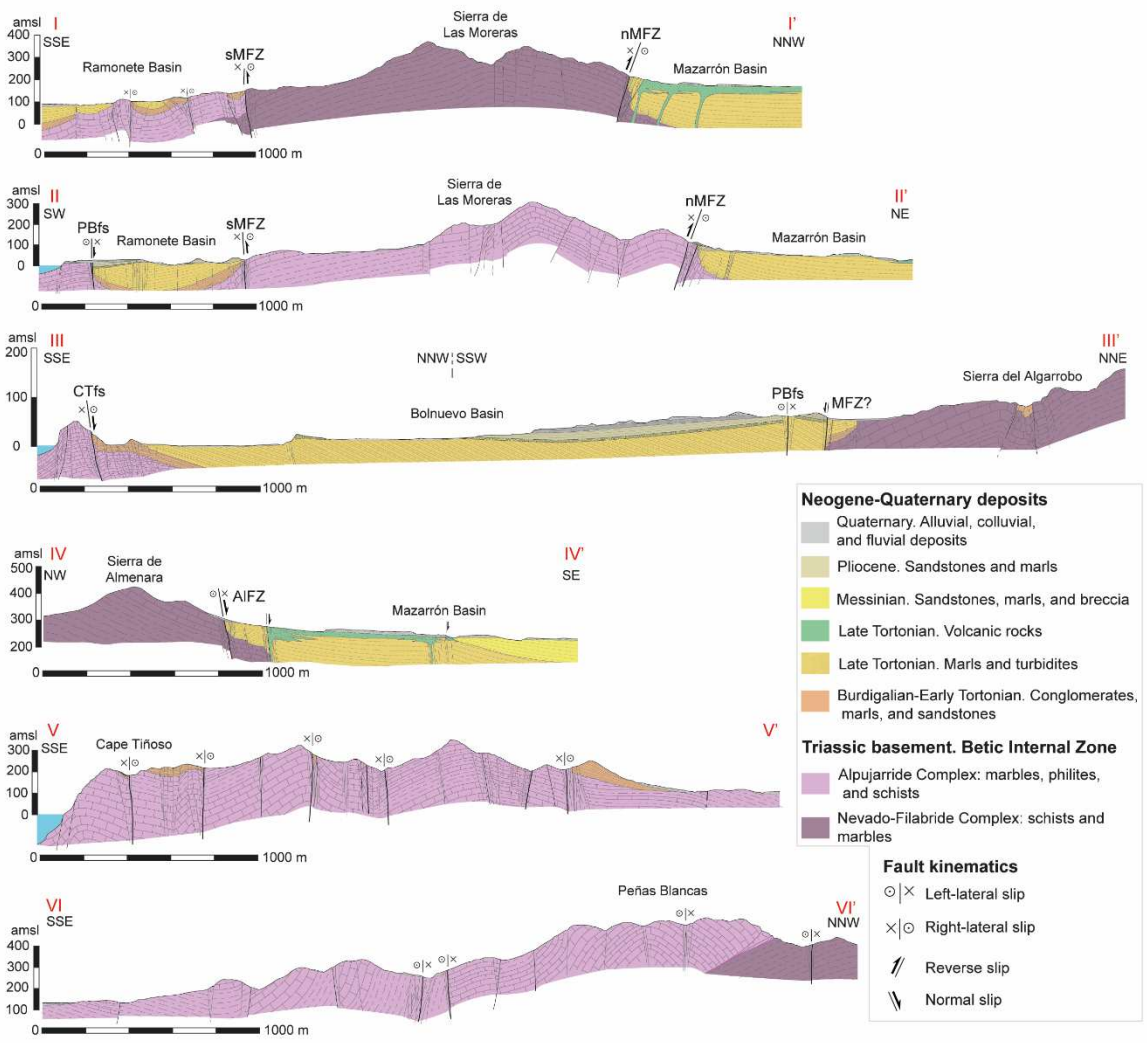


Fig. 4 Geological cross-sections across the main fault zones studied in this work. The position of the sections is indicated in figure 3

The southern MFZ displays slip surfaces dipping vertically, to the NE and to the SW (between ca. 30 to 90º, Fig. 5). This strand is the border fault of the Ramonete basin to the north (Figs. 3 and 4). It deforms the Burdigalian to Tortonian infill deposits of the Ramonete and Bolnuevo basins, that appear intensely deformed (Figs. 6a and 7a, b). On the contrary, deformation is less intense in Messinian and Lower Pliocene deposits, which lie unconformably over the older rocks. Although some of these later deposits are offset by faults, deformation normally consist of gentle tiltings between 10 and 20º, mainly to the south (Fig. 7c). To the west, the southern MFZ diverges into two branches that delimit a small quadrangular basin filled with upper Tortonian marls and large volumes of volcanic rocks (Fig. 3).

In the western sector, the southern MFZ does not appear to be significantly dissected by secondary faults, showing a roughly sublinear mountain front. The southern strand displays a complex fault zone, ten to hundred meters wide (Fig. 6a). It presents an anastomosed pattern on surface, where the basement and basin infill deposits are intensely deformed and pierced within the fault zone, forming lensed-shaped bodies on map view (Fig. 3). In the eastern sector, the southern MFZ shows a saw-like geometry, since it is offset by a set of steep NE-SW (ca. N060E) and N-S faults (Figs. 3 and 5). Consequently, the southern mountain front is very irregular in this sector.

The northern MFZ displays slip surfaces dipping vertically or steeply to the NE (ca. 65º) in the western sector of the fault, while it dips vertical or to the SW (ca. 45º) in the eastern sector (Fig. 5). This strand is the border fault of the Mazarrón Basin to the south (Figs. 3 and 4). It presents a ten of meters wide fault zone, where the Upper Tortonian deposits of the Mazarrón basin are intensely deformed (Fig. 6b). It is also remarkable the large volumes of Upper Tortonian volcanic rocks cropping out adjacent to this fault zone (Figs. 3 and 4). Away from the fault zone, the Tortonian deposits are tectonically tilted ca. 20º to the north, while the Messinian deposits are gently tilted between 15 and 20º, becoming gradually sub-horizontal towards the basin centre (Fig. 4). In the western sector, the trace of the northern MFZ is dissected by secondary N-S, NNW-SSE, and NNE-SSW faults that cut through the basement rocks (Fig. 3). These faults are responsible for the high sinuosity of the northern mountain front. However, towards its eastern termination, the northern MFZ presents a ca. 4 km-long markedly linear segment (Figs. 3).

In this linear segment, the northern MFZ may be affecting two generations of Pleistocene alluvial fans. Marked lineations are observed in these alluvial fans in the historical aerial photographs of this sector (Fig. 8a). However, the available field evidence of these features is scarce since human activity has removed part of the alluvial deposits. On the one hand, a possible offset is observed at the base of one of the oldest fans, composed by boulders with a cemented matrix (Fig. 8b). On the other hand, one of the most recent alluvial fans also appears to exhibit minor deformation. In the outcrop, a secondary strand of the MFZ seems to offset the conglomeratic fan deposits (Fig. 8c).

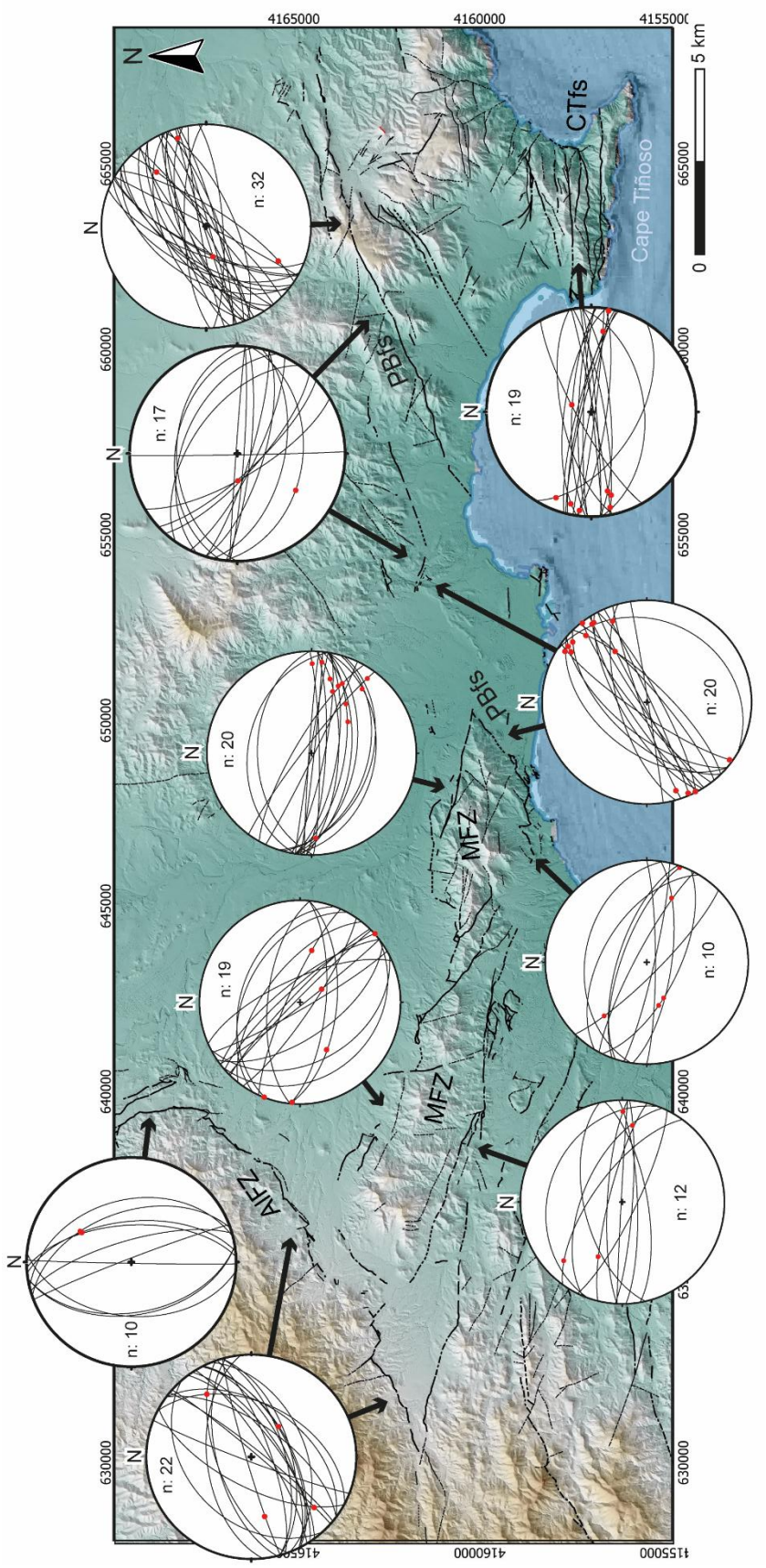


Fig. 5 Map displaying the surface geometry of the studied faults. Stereographic plots depict structural data of fault planes and slickenlines (in red) collected in each structure. MFZ: Moreras Fault Zone; AlFZ: Almenara Fault Zone; PBfs: Peñas Blancas fault system; CTfs: Cape Tiñoso fault system

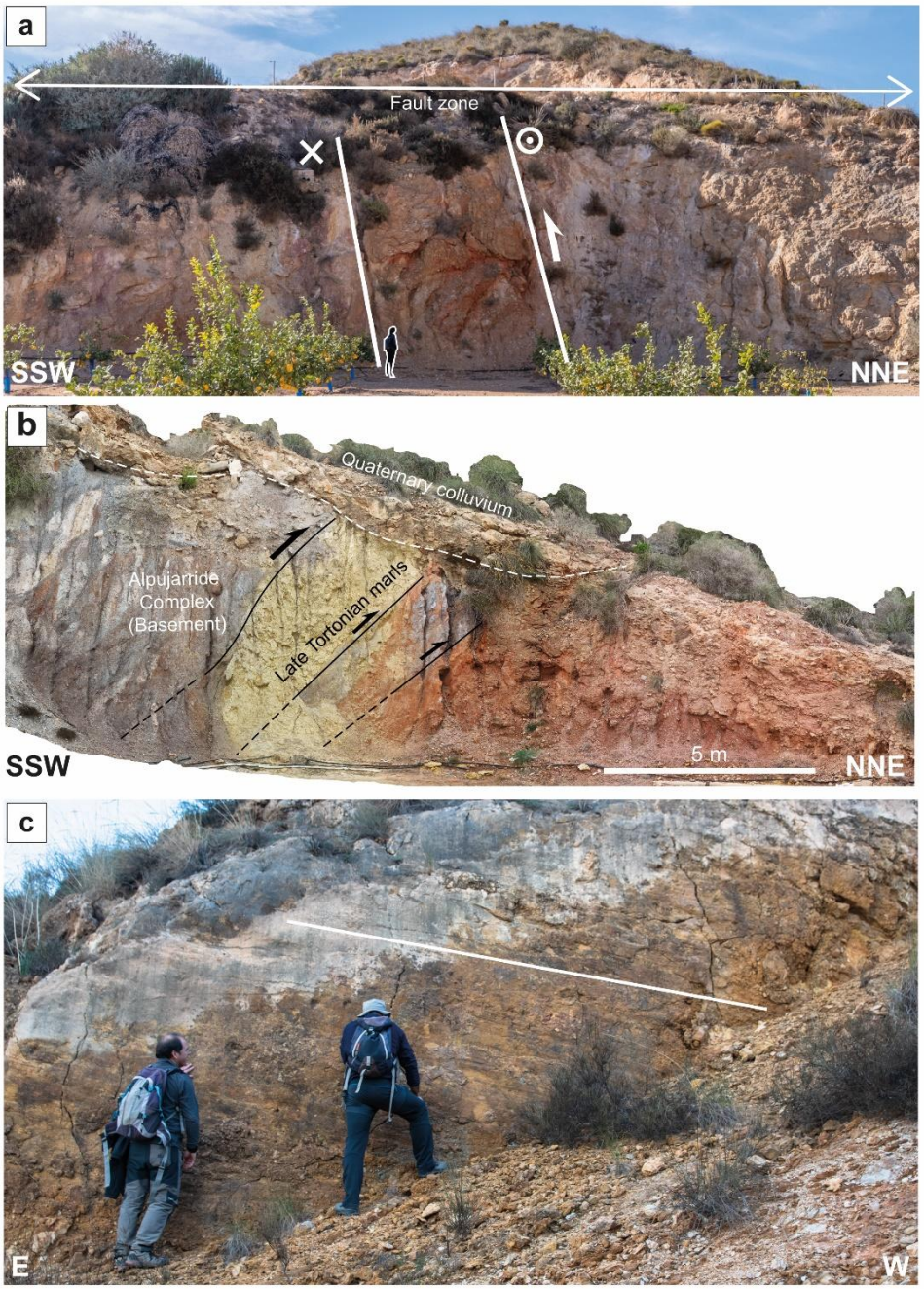


Fig. 6 Pictures of the MFZ. a) Fault zone of the southern MFZ, tens-of-meters wide. The basement rocks and Miocene conglomerates appear highly deformed by this fault strand. Location: 642181.644 m E,4159688.039 m N. b) Main fault zone of the northern MFZ. The basement Alpujarride rocks, in the hanging-wall, are placed over the Upper Tortonian marls and later continental deposits. Location: 648405.049 m E,4160577.000 m N. c) Slickenlines developed in a fault plane in the southern MFZ. Location: 641529.332 m E,4159789.750 m N

The terminations of the MFZ are connected to other faults (Fig. 3). To the west, the northern MFZ appear to terminate against the Almenara Fault Zone at an angle of ca. 80º. However, minor NW-SE faults aligned with the MFZ cut across this fault and offset its mountain front a few hundred meters (Fig. 3). The southern MFZ intersects the Almenara Fault Zone at ca. 35º. From the intersection point, the continuation of the MFZ is not clear, since it appears to cross the reliefs of the Almenara anticline towards the west. However, the expression of this structure is

obscured in the field and can only be deduced from some local outcrops and geomorphic lineations observed in the DEMs.

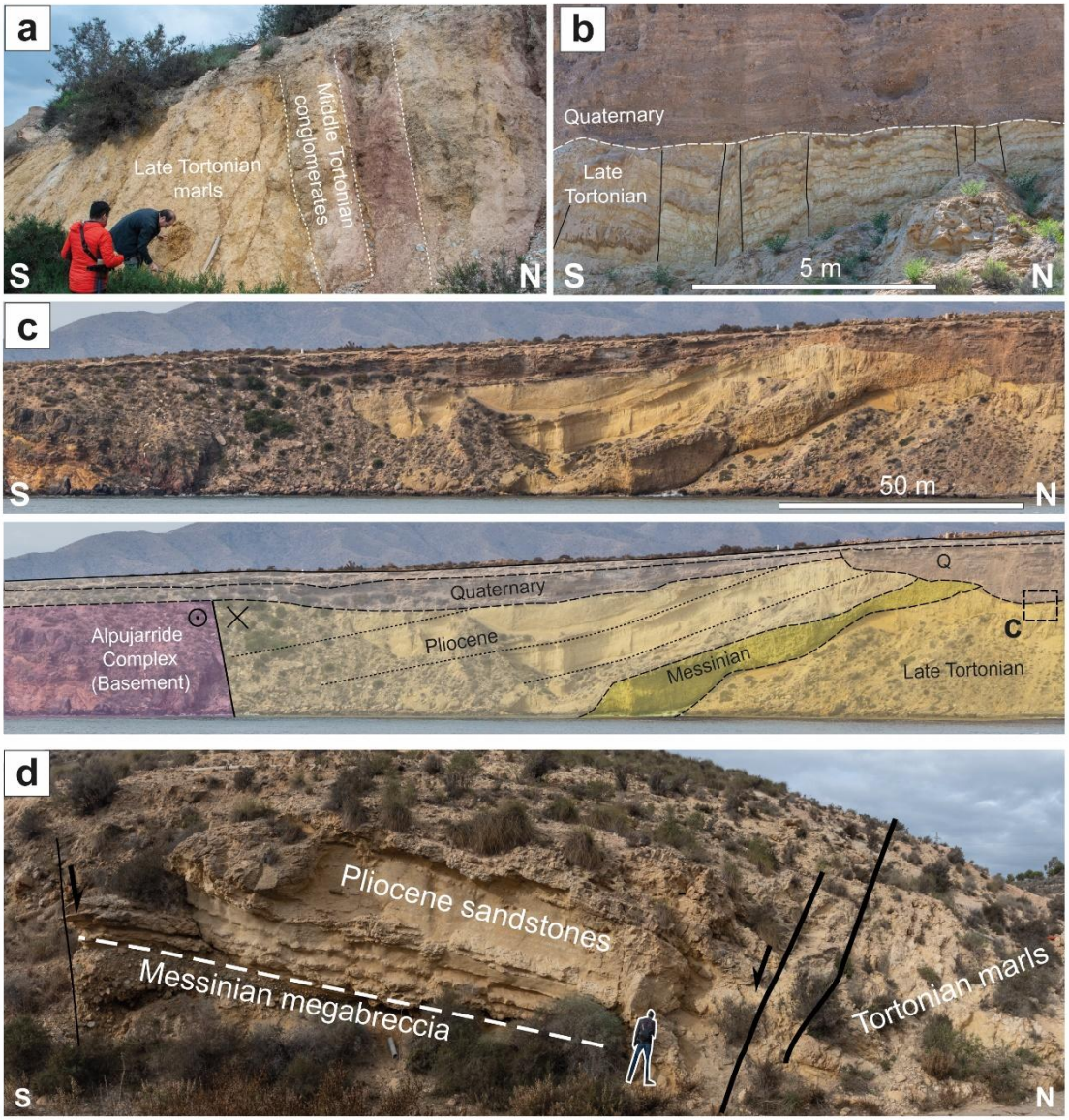


Fig. 7 Tectonic deformation in Neogene deposits along the MFZ. a) Sub-vertical Tortonian deposits by the southern MFZ. Location: 650122.114 m E, 4159228.979 m N. b) Unconformity between highly faulted Upper Tortonian turbidites and sub-horizontal Quaternary alluvial fans. Position of the picture in c) Picture and interpreted section showing the relation between the highly fractured Upper Tortonian (in b), the tilted Messinian and Pliocene, and the sub-horizontal Quaternary deposits. Location: 647274.184 m E, 4158138.629 m N. d) Offset and tilting of Messinian and Pliocene rocks related to a WNW-ESE fault in the northern margin of the Bolnuevo Basin. Location: 653715.129 m E, 4161607.055 m N

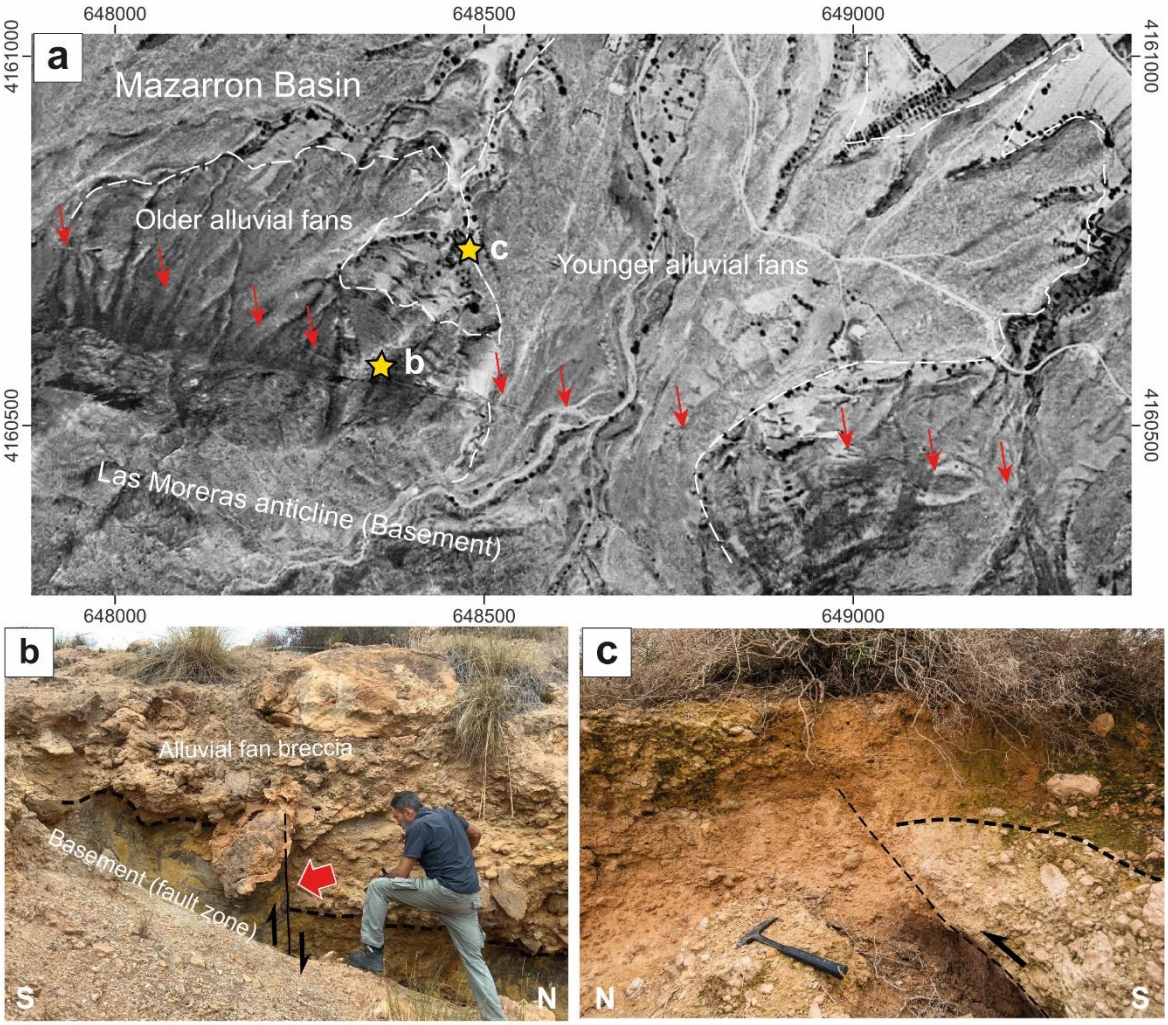


Fig. 8 Geological evidence of deformed Quaternary deposits in the MFZ. a) Historical aerial photography (1956) where clear lineations are observed in different generations of alluvial fans along the northern MFZ. Yellow stars mark the location of outcrops in b) and c). b) Small offsets in the basal breccia of the older generation of alluvial fans. Location: 648352.159 m E, 4160606.157 m N. c) A secondary strand in the northern MFZ subtly deforms one of the most recent alluvial fans. Location: 648464.042 m E, 4160729.567 m N

The eastern termination of the MFZ appears to be intersected by NE-SW faults, which in this study are included in the so called Peñas Blancas fault system (Fig. 3). These structures mark the end of the main surface expression of the fault zone. However, faults with the same orientation of the MFZ can be found in the northern margin of the Bolnuevo Basin and offsetting the basement rocks towards the NE, interacting with the Peñas Blancas and Cape Tiñoso fault systems (Fig. 3). The sedimentary infill of the Bolnuevo Basin is deformed as result of these interactions: Late Tortonian deposits are tilted up to 30º in some locations, while Messinian and Pliocene deposits define a gentle, roughly W-E syncline (Figs. 3 and 5) which northern limb is offset faults (Fig. 7d).

Fault kinematics along the MFZ are reflected mainly by mesoscale kinematic indicators, such as slickenlines (Fig. 6c), and the crosscut relations with other structures. Slickenlines found along the northern main strand display rakes ranging between 1 and 54º SE, with a mean of 28º SE. In the southern main strand, rakes range between 34º NW and 35º SE, with mean values of 33º NW and 21º SE, respectively (Fig. 5). These markers indicate an oblique motion, with a main strike-

slip component. The sense of slip of the strike-slip component and the total displacement produced by the MFZ can be inferred using the contact between the Nevado-Filábride and Alpujárride complexes as a geological marker. This contact traces a roughly continuous arched geometry in map view along the Águilas Arc (García-Tortosa *et al.*, 2000; García-Tortosa, 2002; García-Tortosa and Leyva, 2004a; Booth-Rea *et al.*, 2008 and 2009), consistent with the regional structural orientations (Fig. 2). However, this trace is offset by the MFZ approximately 10 km in a right-lateral sense, of which about ca. 6 km correspond to the southern main strand (Fig. 3). Additionally, the faults forming the MFZ produce smaller offsets in the Las Moreras anticline and in the mountain front of the Almenara Fault Zone (Fig. 3), also pointing to a right-lateral sense of displacement, which is consistent with the descriptions of De Larouzière *et al*. (1987) and Coppier *et al*. (1989).

3.2. The Almenara Fault Zone

The Almenara Fault Zone extends about 13 km with a N060E strike, bounding the Mazarrón Basin to the west (Fig. 3). The fault zone is formed by slip surfaces dipping between ca. 45º and 85º to the SE (Figs. 5 and 9a), although antithetic faults can be found along its trace. It offsets the SE limb of the N060E Almenara anticline, formed by rocks of the Nevado-Filábride complex (García-Tortosa, 2002) (Figs. 3 and 4). The fault zone deforms the Upper Tortonian and Messinian infill of the basin, including the volcanic rocks that intruded subparallel to the fault trace (Fig. 3). The basin deposits are generally tilted ca. 20 to 25º towards the east, but their dips increase to ca. 45-50º near the fault zone (Figs. 3 and 5). Evidence of deformation within Quaternary deposits is very scarce along the Almenara Fault Zone. The most clearly exposed outcrop is located near the SW termination of the fault zone (Fig. 9b). Here, Pleistocene alluvial deposits, formed by reddish silts and breccia, appear offset by faults. Slip surfaces with slickenlines can be observed within these alluvial deposits (Fig. 9c).

Towards the SW, the trace and mountain front of the Almenara Fault Zone is dissected and offset by secondary faults of the MFZ (Fig. 3). The main surface expression of the Almenara Fault Zone terminates against the MFZ, although it produces a small offset in this fault of ca. 1 km. In the past, the fault zone may have extended toward the SW, following former intrabasement contacts until it reached the N020E Terreros or Palomares faults. However, this cannot currently be determined based on field observations. On the other hand, the NE termination is marked by N-S to NNW-SSE normal faults (Figs. 3 and 5) related to the formation of the Mazarrón Basin during the late Tortonian (De Larouzière *et al*., 1987; De Larouzière and Ott d'Estevou, 1990).

Regarding fault kinematics, slickenlines along the main strands of the Almenara Fault Zone are scarce, displaying rake values ranging between 23 and 80º −predominantly SW− that reflect an oblique-slip motion, with a normal and a strike-slip components (Figs. 5 and 9c, d). The sense of horizontal displacement could be deduced from the offset produced in the western termination of the MFZ, which suggests a left-lateral motion. This would be consistent with the kinematics proposed by Coppier *et al*. (1989) and De Larouzière and Ott d'Estevou (1990).

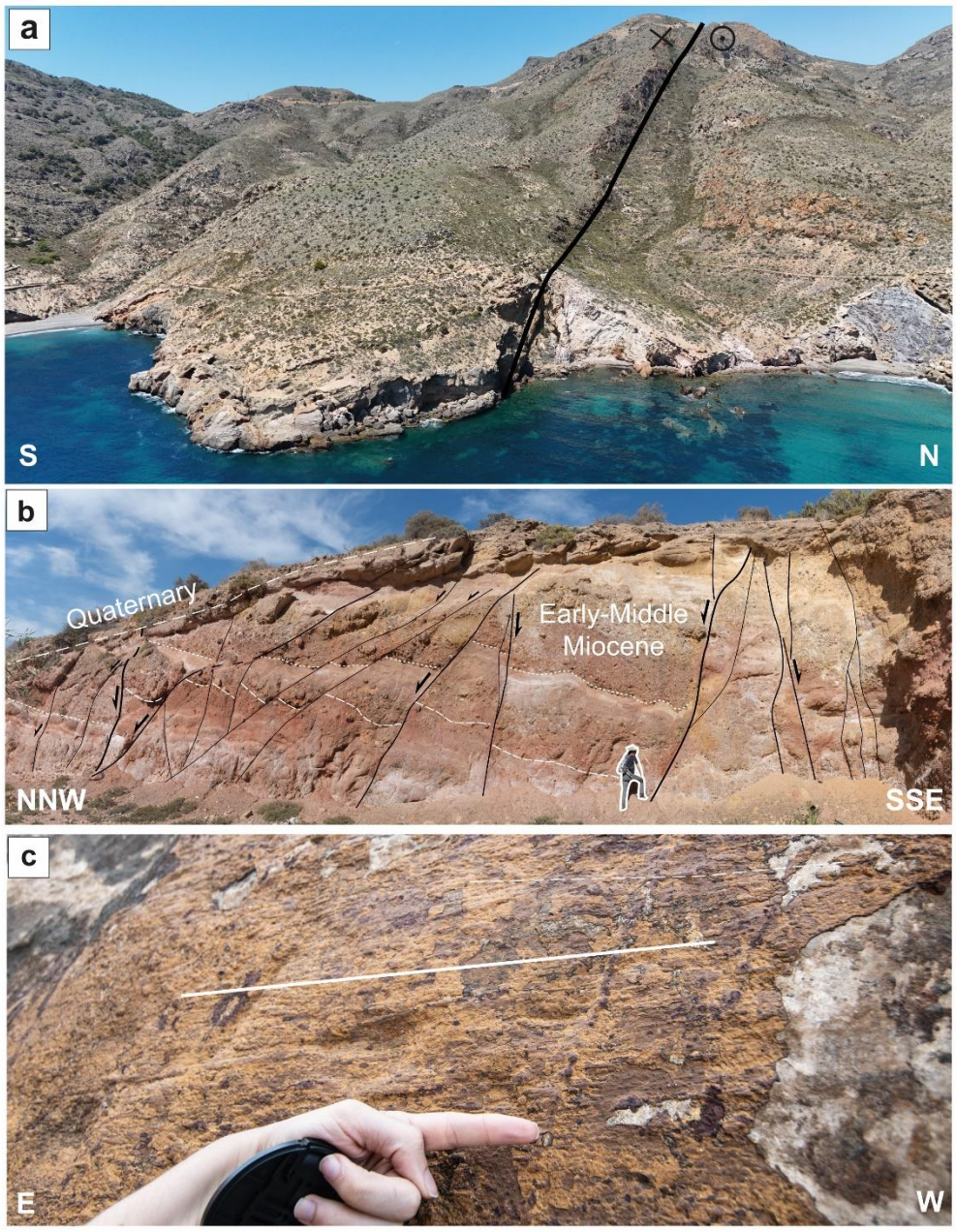


Fig. 9 Pictures of the Almenara Fault Zone. a) Fault plane with the basement Nevado-Filabride rocks in the footwall and Upper Tortonian marls in the hanging-wall. Location: 638805.151 m E, 4166870.586 m N. b) Offset Quaternary alluvial fan conglomerates near the southern termination of the Almenara Fault Zone. Location: 630315.268 m E, 4161642.600 m N. c) and d) Slickenlines found in faults planes along the Almenara Fault Zone

3.3. The Cape Tiñoso fault system

The Cape Tiñoso fault system extends approximately 15 km with a main N090E direction across the reliefs of Cape Tiñoso and the south of the Bolnuevo Basin (Figs. 3 and 10a). In Cape Tiñoso,

366 the fault system is formed by subparallel major fault zones with sublinear surface traces that
367 offset the folded basement rocks of the Alpujarride complex (Figs. 3 and 4).



368

369 **Fig. 10** Pictures of the Cape Tiñoso fault system. a) W-E fault zone offsetting the basement rocks of the
370 Alpujarride Complex in Cape Tiñoso. Location: 665495.343 m E, 4157662.618 m N. b) Intensely faulted
371 Burdigalian conglomerates near a W-E fault zone. Location: 653587.943 m E, 4158450.884 m N. c) Sub-
372 horizontal slickenlines found in a W-E fault plane. Location: 663734.712 m E, 4158627.863 m N

373 Faults are subvertical or dip steeply to the north and south (Fig. 5). The separation between
374 these main structures ranges from ca. 400 m to ca. 1000 m. The fault zones are well developed,
375 reaching thicknesses of tens of meters. They have a marked geomorphological expression,
376 forming narrow and rectilinear W-E ridges and corridors (Fig. 10a). The W-E faults of the Cape
377 Tiñoso fault system are intersected by NE-SW faults belonging to the Peñas Blancas fault system
378 and WNW-ENE faults (Fig. 3).

The Cape Tiñoso fault system mainly deforms the basement rocks, since Neogene sedimentation is very scarce (Fig. 3). However, Burdigalian to Early Tortonian conglomerate deposits appear pierced, offset, or tilted northwards by these faults in some locations. Moreover, the E-W faults extend towards the west across the Gulf of Mazarrón, as observed in available seismic profiles (ITGE, 1990). They crop out again in the southern margin of the Bolnuevo Basin, juxtaposing the basement Alpujarride rocks and the Neogene sedimentary infill of the basin (Fig. 3). The Burdigalian deposits in this margin appear intensely faulted by this fault system (Fig. 10b). Slickenlines found on the W-E fault surfaces show rakes between 2 and 25º (predominantly W) (Figs. 5 and 10c), indicating a major strike-slip component.

3.4. The Peñas Blancas fault system

The Peñas Blancas fault system is formed by faults with a mean N060E strike that extends a minimum of 22 km (Fig. 3). The fault system consists of a broad ca. 8 km-wide band formed by subparallel fault zones with roughly rectilinear surface traces (Fig. 3). Faults display vertical or highly dipping planes to the NW and to the SE (Figs. 4 and 5). There are three main fault strands, in terms of length and the deformation they produce. Some of these strands present well-developed fault zones, up to 600 m-wide (Fig. 4 and Fig. 11a). Spacing between main fault strands varies from hundreds of meters to ca. 1.5 km. Other faults striking WNW-ENE, analogous to the MFZ, exhibit mutual cross-cut relations with the Peñas Blancas faults.

Terminations of this fault system are obscured in the field. Towards the NE, the main fault strands coalesce into a ca. 1 km-wide fault zone, which surface expression terminates when it is covered by the quaternary alluvial systems of the Campo de Cartagena Basin (Fig. 3). However, this fault zone is relayed by a N070E major fault located to the south, forming a ca. 2.5 km right stepover. This structure extends along the southern margin of the Campo de Cartagena Basin (Manteca-Martínez *et al.*, 2004). On the other hand, faults of the Peñas Blancas system extend towards the SW cropping out in the southern and western margins of the Bolnuevo Basin (Fig. 3). Faults in the western margin are those intersecting the MFZ and likely extend southwestward beneath the sea.

The Peñas Blancas fault system deforms mainly the folded basement rocks of the Nevado-Filábride and the Alpujárride complexes (Figs. 4 and 11a, b). However, it also affects the sedimentary infill of the Bolnuevo Basin: middle Miocene to Tortonian deposits present a high degree of deformation, being offset and tilted up to 40º (Fig. 11c), while offsets in Messinian and Pliocene deposits are subtler (Fig. 4). Evidence of Quaternary deformation is scarce, consisting of local vertical fabrics and fractures affecting colluvial breccia deposits (Fig. 11e).

Slickenlines in the Peñas Blancas fault system were mostly found in the faults that offset the MFZ to the east (Figs. 5 and 11d). These indicators display rakes ranging from 1º SW and 42º NE, with mean values of 4º SW and 12º NE, respectively. Thus, they reflect a predominant strike-slip component. Moreover, the offsets produced by these faults in the contacts between the basement and the basin infill deposits suggest a left-lateral sense of slip, which is also supported by previous studies (Montenat and Ott d'Estevou, 1987; Montenat et al., 1987) and recent GNSS data (Khazaradze *et al*., in press).

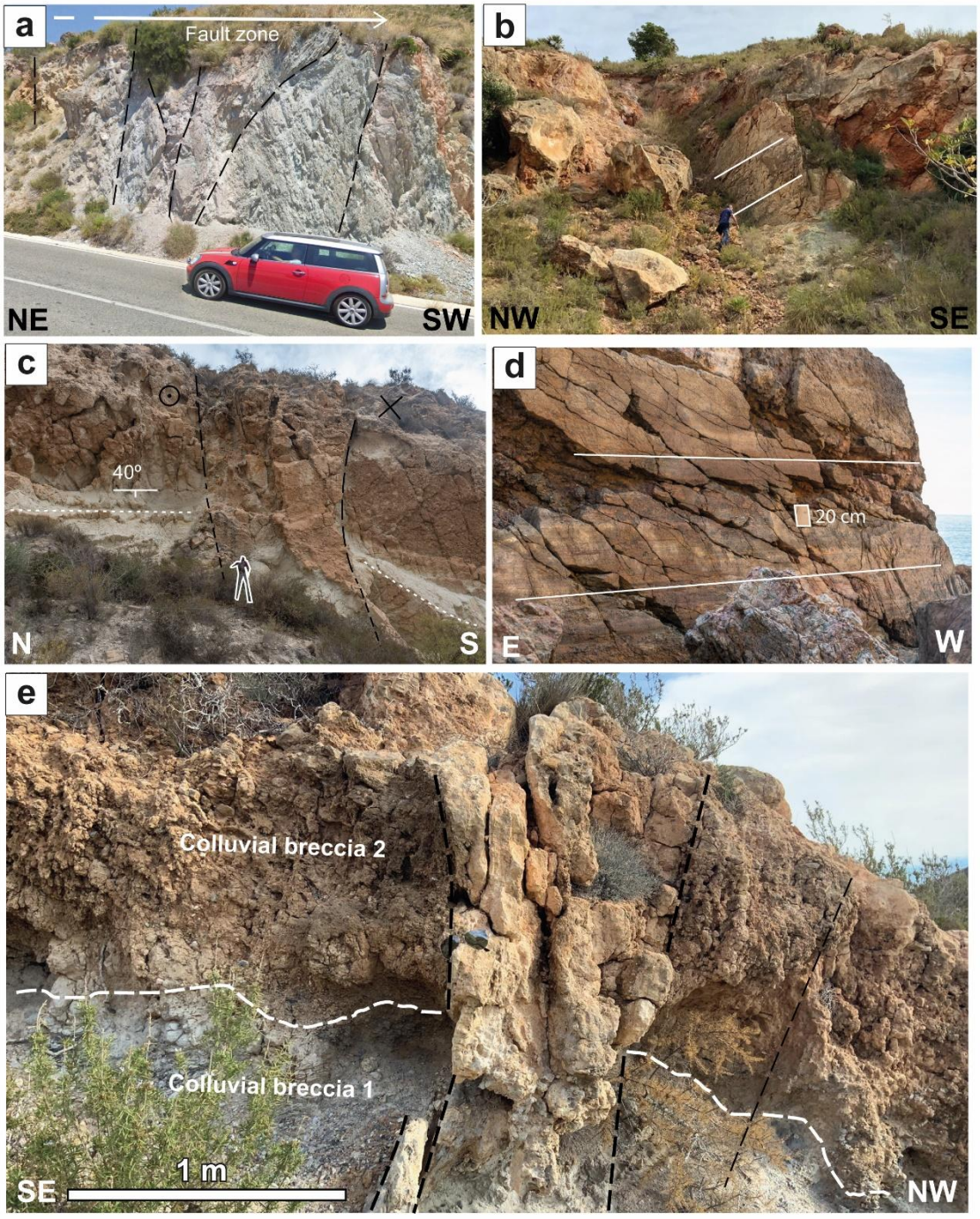


Fig. 11 Pictures of the Peñas Blancas fault system. a) and b) NE-SW fault zones offsetting the basement rocks of the Alpujarride Complex. Location of a: 662754.661 m E, 4161454.093 m N. Location of b: 660874.327 m E, 4162332.087 m N. c) Fault zone offsetting Upper Tortonian rocks in the Bolnuevo Basin. Location: 653814.640 m E, 4161326.792 m N. d) Sub-horizontal slickenlines in a NE-SW fault plane. Location: 648757.315 m E, 4158605.208 m N. e) Deformation in Quaternary colluvial deposits aligned with a NE-SW fault of the Peñas Blancas fault system. Location: 661993.690 m E, 4162924.912 m N

4. Discussion

The MFZ is currently classified as a structure with activity during the Quaternary (García-Mayordomo *et al*., 2012; García-Mayordomo and Martin-Banda, 2022). However, its activity

during the Late Pleistocene - Holocene, i.e., during the last 129 kyr, has not been demonstrated yet. The new geological and structural data presented in this study allow to revise the geometry, extent, and tectonic significance of the MFZ. In particular, the discussion focuses on two main issues. First, it re-evaluates the total length of the fault and its relationship with other structures in the Águilas Arc and in the Mazarrón Escarpment. Second, it examines the Quaternary activity of this sector and the implications for the tectonic evolution of the Eastern Betic Cordillera.

4.1. A revision of the total length of the Moreras Fault Zone

The total length of the MFZ has been revised several times since the structure was first described. The first map and mention of the fault was provided by De Larouzière *et al*. (1987) and described later by Coppier *et al*. (1989). In these works, the fault zone consists of two N100E main faults that bound the Las Moreras range to the north and south for about 22 km. Moreover, Coppier *et al*. (1989) also inferred that the southern MFZ could continue 6 km to the west across the Almenara anticline, connecting with the faults of the EBSZ, and 4 km to the east through the Bolnuevo Basin. Considering these works, the onshore segment of the MFZ would be approximately 32 km long (Fig. 12a).

Additionally, several authors have described offshore segments of the MFZ. The first mention of the offshore segment of the MFZ can be also found in Coppier *et al*. (1989). In their study, the authors used bathymetric and magnetic data to describe the main structural features of the continental margin in SE Spain. From these data, they interpreted structural features with N090E to N110E trends that control the orientation of the Mazarrón Escarpment south and west of Cape Tiñoso (Fig. 12). Consequently, these authors also included the faults of the Cape Tiñoso fault system as part of the MFZ. Subsequent studies described the continuation of the MFZ as a ca. 10 km-wide fault zone extending about 30 km to the east along the continental shelf (ITGE, 1990; Díaz del Río, 1991; Acosta *et al.*, 2013). In these studies, they also defined a series of offshore NW-SE to SW-NE structures along the Mazarrón Escarpment, with interpreted right-lateral and left-lateral kinematics, respectively (Fig. 12).

Based on these previous observations, the MFZ is often considered as a segment of a larger structure, the Moreras- Mazarrón Escarpment, that includes all these offshore faults (García-Mayordomo, 2005; García-Mayordomo *et al*., 2012) (Fig. 12a). Considering all these segments, the length of this structure would be of approximately 100 km.

However, the updated structural characterization of the MFZ and other faults carried out in the present study does not support this idea. Alternatively, it partially corroborates the first descriptions presented by De Larouzière *et al*. (1987) and Coppier *et al*. (1989), i.e., that the onshore MFZ extends north and south of the Las Moreras Range and may continue west of the Almenara Fault Zone for at least 3 km (Fig. 12b). However, there are several evidence that does not support an eastward continuation of the MFZ to Cape Tiñoso. First, the faults forming the Cape Tiñoso fault system exhibit orientations different from those of the MFZ (Figs. 3 and 5), and therefore are unlikely to form part of the same fault zone. Second, the observed crosscutting relationships indicate that the MFZ terminates to the east against the NE-SW faults of the Peñas Blancas fault system. Considering the left-lateral motion of the Peñas Blancas fault system described in this and previous studies (Montenat and Ott d'Estevou, 1987; Montenat *et al.,* 1987; Khazaradze *et al*., in press), the eastern continuation of the MFZ should have been offset and displaced towards the NE, being disconnected from the rest of the fault zone (Fig. 12b). This left-lateral offset of the MFZ would be consistent with the presence of WNW-ESE faults in the northern margin of the Bolnuevo Basin (Fig. 3) and to the east of Cape Tiñoso (Acosta *et al*.,

2013) (Fig. 12b). Moreover, some of the segments included as part of the Moreras-Mazarrón Escarpment structure are interpreted as left-lateral faults (segment 3 in Fig. 12a) in contrast to the right-lateral kinematics proposed for the other segments.

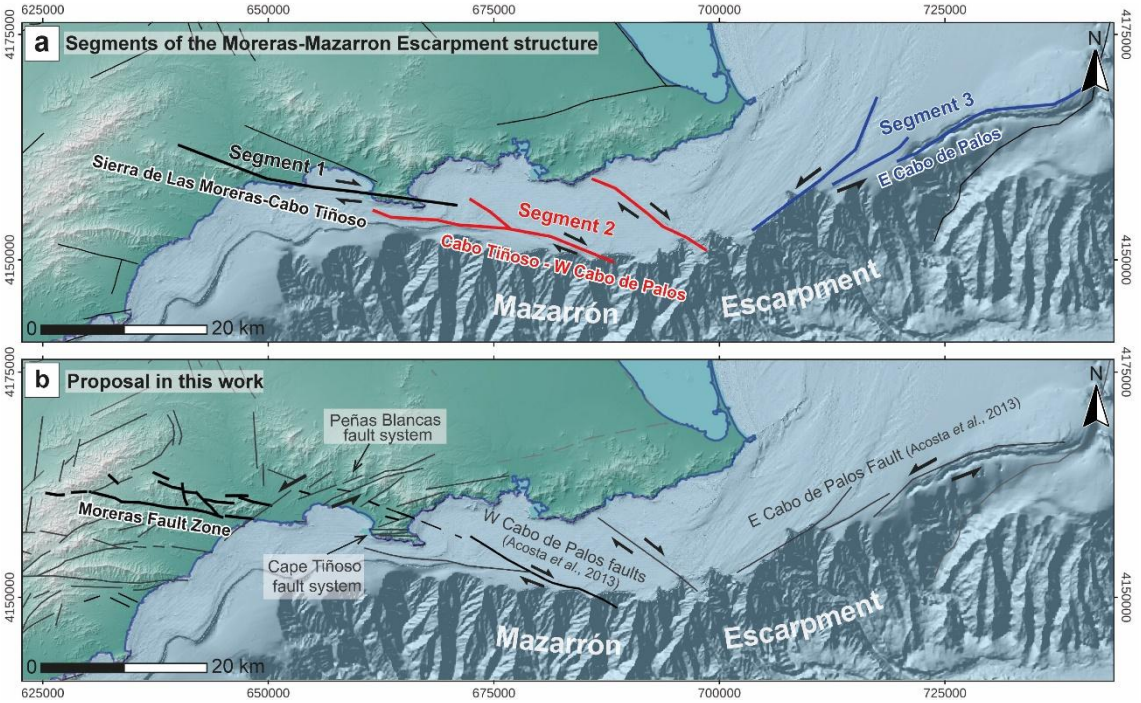


Fig. 12 a) Trace map of the Moreras-Mazarrón Escarpment structure as currently included in the QAFI database (García-Mayordomo *et al.*, 2012), which is based on previous studies (De Larouziere *et al.*, 1987; Coppier *et al*., 1989; ITGE, 1990; Díaz del Río, 1991; García-Mayordomo, 2005; Acosta *et al.*, 2013). The MFZ is included as a segment of this structure (Sierra de Las Moreras-Cabo Tiñoso segment) together with two offshore segments (Cabo Tiñoso-West Cabo de Palos and East Cabo de Palos segments). b) Trace map illustrating the interpretation proposed in the present study: the MFZ is interpreted as a structure distinct from the Cape Tiñoso fault system and is disconnected from the other WNW-ESE faults due to the offset produced by the Peñas Blancas fault system. The offshore structures identified by Acosta *et al*., 2013 are also interpreted as separated faults

Taking all these observations into account, the faults at Cape Tiñoso and the Mazarrón Escarpment should be considered distinct from the MFZ (Fig. 12b). Therefore, the MFZ would extend for only approximately 23 km, terminating in the Bolnuevo Basin, where it is offset by the Peñas Blancas fault system. From a seismogenic approach, this redefinition may be significant, since it substantially limits potential rupture lengths and thus maximum expected earthquakes.

4.2. Quaternary activity of the Moreras Fault Zone and related faults

Most faults in the study area likely accommodated deformation since the early-middle Miocene, during the initial structuration of the Águilas Arc (De Larouzière *et al*., 1987; Coppier *et al*., 1989). Crosscutting relationships between SW-NE, W-E, and WNW-ENE faults suggest contemporaneous activity at some point, although the main deforming structures may have varied, implying kinematic changes over time. In general, tectonic activity was more intense during the early stages. This is evidenced by the angular unconformities between lower Miocene to upper Tortonian deposits, displaying higher dips, and Messinian and Pliocene deposits, which

tilting is gentler (Figs. 3, 4, and 7). Moreover, Messinian and Pliocene faulting is very local along the study area (Fig. 7d).

During the Quaternary, the MFZ may have accommodated less deformation than in Neogene times. The evidence used to classify the MFZ as active during the Quaternary consists of indirect criteria, such as estimates of the differential uplift between the Las Moreras range and the Ramonete Basin during the Early and Middle Pleistocene (Bardají, 1999). Other evidence is the seismicity in the region. This seismicity is very low, characterized by the occurrence of occasional low-magnitude earthquakes. The most remarkable event is the 1996 Mazarrón seismic series (Martinez-Solares and Mezcua, 2002). This seismic series was characterized by a main event with a magnitude of 4.5 and an intensity of V, followed by eight aftershocks with magnitudes between 2.5 and 3.5. Based on the roughly WNW–ESE alignment of the epicenters, García-Mayordomo (2005) proposed the MFZ as a potential seismic source. However, this evidence is weak, as the event locations (Fig. 2) suggest they are more likely associated with the Terreros Fault.

In contrast, García-Tortosa and Leyva (2004a) point to the low linearity of the mountain front as evidence of low or absent Quaternary activity in most of the MFZ. These authors expose only two possible evidences of recent activity in local sectors of the MFZ. One is the higher mountain front linearity and tectonic geomorphic features (anomalies in the drainage network geometry and triangular facets) found in the easternmost sector of the northern MFZ. The other is the existence of iron mineralizations affecting Pleistocene marine and continental deposits near the southern MFZ. They argue that these mineralizations, together with high temperatures registered in boreholes near the fault zone (ITGE, 1993), could be an indirect indicator of fault activity.

In the present study, a special emphasis was placed on searching for geological evidence of Quaternary deformation along the fault zones in the study area. However, this evidence is subtle and very scarce. In the MFZ, only two outcrops were found in the easternmost sector of the northern strand, where alluvial fan deposits seem slightly affected (Fig. 8b, c). This would be reinforced by the lineations observed in these fans in historical aerial photographs (Fig. 8a). Moreover, it would be consistent with the signs of Quaternary activity suggested by García-Tortosa and Leyva (2004a) for this sector. The same applies to the Almenara Fault Zone and the Peñas Blancas fault system, where direct Quaternary deformation features are very limited to local outcrops (Figs. 9b and 11e).

The scarce geological evidence of recent deformation, as well as the lack of geomorphological signature (García-Tortosa and Leyva, 2004a), and the low seismicity in the region could be explained by a significant decrease in the tectonic activity of the faults of this sector of the Águilas Arc during the Pliocene but especially during the Quaternary. In contrast, Plio-Quaternary deformation and seismicity documented in the faults forming the EBSZ to the north is considerably higher (e.g., Booth-Rea *et al*., 2003; Masana *et al*., 2004; Alfaro *et al*., 2012; Martínez-Díaz *et al*., 2012; Martín-Banda *et al*., 2016; Martin-Rojas *et al*., 2015). This suggests a northwards migration of the deformation accommodated within the tectonic arc during the Messinian – Early Pliocene.

However, the faults in the Águilas Arc still appear to present a certain degree of activity at present. A recent study (Khazaradze *et al*., in press) has unravelled, from new GNSS data, the amount of tectonic deformation that is currently being accommodated in the Águilas Arc. Their results indicate that, along a NNW-SSE transect that includes the WNW-ESE MFZ, the SW-NE Almenara Fault Zone, the Ramonete Fault, and the W-E Lomo de Bas Fault (Fig. 2), a cumulative

549 horizontal shortening of 0.4±0.1 mm/yr is accommodated, while the strike-slip deformation
550 is non-significant (0.0±0.1 mm/yr). Although it is not possible to attribute these rates to one
551 or more specific fault, these data could imply a certain degree of tectonic activity in some of the
552 faults of the study area, such as the MFZ or the Almenara Fault Zone. Nevertheless, these rates
553 suggest that, if these faults are active, their strike-slip motion is currently inhibited. In the case
554 of the MFZ, the right-lateral displacement reflected by geological markers (Fig. 3) and described
555 by Coppier *et al*. (1989) may be arrested at present. On the other hand, according to Khazaradze
556 *et al*. (in press), to the east of the study area deformation would be accommodated by
557 transpresive structures, with a left-lateral slip rate of 0.6±0.1 mm/yr and a shortening rate of
558 0.4±0.1 mm/yr. Faults within the Peñas Blancas fault system could be partially absorbing this
559 deformation. These data also support a northward migration of the deformation, since slip rates
560 in the EBSZ range from a minimum of 0.3 to up to 1.3 mm/yr (Echeverria *et al.*, 2013 and 2015;
561 Borque *et al.*, 2019; Portela *et al*., 2025).

562 The lack of robust Quaternary indicators revealing this deformation could be also related to the
563 poor outcrop conditions of Quaternary deposits along the studied faults. The marine regression
564 during the late Messinian and early Pliocene (Montenat, 1975; De Larouziere *et al.* 1987; De
565 Larouzière and Ott d'Estevou, 1990) restricted the continental sedimentation to semiarid alluvial
566 fans and fluvial systems that have been subjected to erosion during all the Late Pliocene and
567 Quaternary, hindering the preservation of proper sedimentary records. Moreover, the intense
568 human activity in the region, specifically the extensive agriculture, have removed a large part of
569 the recent Quaternary deposits. These two factors could have contributed to the obliteration of
570 potential evidence of deformed Quaternary deposits.

571

572 **5. Conclusions**

573 This study presents a new geological and structural characterization of the Moreras Fault Zone
574 (MFZ) and the main associated faults of the northern Águilas Arc. The provided data allow to
575 update the fault geometries, kinematics, structural relationships, and to reassess the tectonic
576 significance of these structures in terms of Neogene-Quaternary activity.

577 The MFZ is a complex fault zone approximately 23 km long and up to 2.8 km wide, formed by
578 two major N105E fault strands and multiple secondary faults that together define a duplex-like
579 structure. Kinematic indicators and geological markers support the kinematics defined by
580 previous authors for this structure, indicating a predominant right-lateral motion and a
581 secondary reverse component. The estimated cumulative horizontal displacement is of about 10
582 km. However, considering recent geodetic studies, these observations may be reflecting the
583 kinematics of the fault during the Miocene, whereas at present it may be acting solely as a
584 reverse fault with a very low deformation rate.

585 The MFZ is related with other faults in this sector of the Águilas Arc. Its western termination
586 shows mutual crosscutting relationships with the N060E Almenara Fault Zone, which presents
587 oblique kinematics with a main left-lateral component. The eastern termination of the MFZ is
588 truncated and displaced by the left-lateral Peñas Blancas fault system, formed by several N060E,
589 subparallel major faults. Finally, the Cape Tiñoso fault system, previously considered as the
590 eastern continuation of the MFZ, has been interpreted as a different structure based on its N090E
591 strike and the structural relations with the other faults. Consequently, the MFZ would also not
592 be connected to the offshore faults of the Mazarrón Escarpment. Consequently, the previously

considered ca. 100 km-long Moreras–Mazarrón Escarpment aggrupation should be regarded as independent fault systems rather than as a single continuous seismogenic structure.

Geological deformation produced by the studied faults was significantly more intense during the Miocene, when they controlled the architecture of the tectonic arc and the sedimentary basins. A decrease in deformation intensity is reflected by the lower tilting and faulting affecting Messinian and Pliocene deposits. Moreover, evidence of Quaternary activity is scarce and restricted to local sectors along the MFZ, consisting of subtle deformation affecting Pleistocene alluvial fan deposits. Comparable limited evidence is observed along the Almenara Fault Zone and the Peñas Blancas fault system, while deformation in the Cape Tiñoso fault system seems restricted to the Neogene.

These observations, together with the low seismicity and the low geodetic slip rates calculated recently in the region, suggest that a small part of the present-day shortening is still accommodated in the Águilas Arc. However, they also point to a progressive migration of the deformation within the Internal Zone of the Eastern Betic Cordillera, from the Águilas Arc towards the Eastern Betic Shear Zone during the latest Neogene and Quaternary. Beyond refining the tectonic evolution of the SE Betic Cordillera, these findings have implications for regional seismic source characterization, as the shorter length proposed for the MFZ and the scarce evidence of Quaternary activity may reduce the seismic potential compared with previous models.

Aknowledgements

This work is part of the project Tectónica Activa del litoral de la Región de Murcia (PID2021-127967NB-I00), funded by the Spanish Ministry of Science, Innovation, and Universities. Partial funding was also provided by the Institut Cartogràfic Valencià, Agencia Valenciana de Seguridad y Respuesta a las Emergencias (Generalitat Valenciana), Consorcio Provincial para el servicio de Prevención y Extinción de Incendios y Salvamento de Alicante, Excelentísimas Diputaciones Provinciales de Alicante y Castellón, and the Ayuntamiento de Almoradí.

Funding and declaration of competing interests

This study was funded by the Spanish Ministry of Science, Innovation, and Universities as part of the project Tectónica Activa del litoral de la Región de Murcia (PID2021-127967NB-I00). Moreover, partial financial support was received from the Institut Cartogràfic Valencià, Agencia Valenciana de Seguridad y Respuesta a las Emergencias (Generalitat Valenciana), Consorcio Provincial para el servicio de Prevención y Extinción de Incendios y Salvamento de Alicante, Excelentísimas Diputaciones Provinciales de Alicante y Castellón, and the Ayuntamiento de Almoradí. Finally, the authors have no competing interests to declare that are relevant to the content of this article.

References

Acosta, J., Fontán, A., Muñoz, A., Muñoz-Martín, A., Rivera, J., Uchupi, E. (2013) The morpho-tectonic setting of the Southeast margin of Iberia and the adjacent oceanic Algero-Balearic Basin.

Marine and Petroleum Geology 45, 17-41. DOI: https://doi.org/10.1016/j.marpetgeo.2013.04.005.

Alfaro, P., Andreu, J. M., Bartolomé, R., Borque, M. J., Estévez, A., García-Mayordomo, J., García-Tortosa, F.J., Gil, A.J., Gràcia, E., Lo Iacono, C., Perea, H. (2012). The Bajo Segura Fault Zone: Active blind thrusting in the Eastern Betic Cordillera (SE Spain). *Journal of Iberian Geology*, 38(1), 271–284. DOI: https://doi.org/10.5209/REV_JIGE.2012.V38.N1.39217

Álvarez-Lobato, F. (1987) *La tectónica de la Zona Bética en la región de Aguilas.* PhD Thesis. Universidad de Salamanca. 371 pp.

Álvaro, M., García-Argüeso, J.M., Elizaga, E. (1975). La estructura del Borde Prebético en la zona de Alcaraz (Provincia de Albacete, España). *Boletín Geológico y Minero* 86 (V): 467-477.

Andrieux, J., Fontbote, J.-M., Mattauer, M. (1971) Sur un modele explicatif de l'arc de Gibraltar. *Earth and Planetary Science Letters* 12 (2), 191-198. DOI: https://doi.org/10.1016/0012-821X(71)90077-X

Andrieux, J. and Nebbad, F. (1996). El prisma orogénico prebético. *Geogaceta*, 20(4): 810-812.

Azéma, J., Foucault, A., Foucarde, E., García-Hernández, M., González-Donoso, J. M., Linares, D., López-Garrido, A. C., Rivas, P., Vera, J. A. (1979) *Las microfacies del Jurásico y el Cretácico de las Zonas Externas de las Cordilleras Béticas*. Secret. Publ. Univ. Granada, 83 pp.

CNIG (Centro Nacional de Información Geográfica) Downloads Centre. https://centrodedescargas.cnig.es/CentroDescargas/index.jsp. (Accessed 30 October 2024).

Baena, J., Álvarez, F., Bardají, T., Calvo, J.P., Elizaga, E., Goy, J.L., Rodríguez-Fernández, J., Santisteban, C., Silva, P.G., Somoza. L., Zazo, C. (1993) *Mapa Geológico de la Comunidad Autónoma de la Región de Murcia E 1:200.000*. IGME-CARM.

Baena-Perez, J.; Moreno-Serrano, F.; Nozal-Martin, F.; Alfaro-Zubero, J.A., Barranco-Sanz, L.M. (1998). *Mapa neotectónico de España*. Madrid, IGME.

Bardají, T. (1999). *Evolución geodinámica de las cuencas neógenas del litoral de Murcia y Almería durante el cuaternario*. PhD Thesis, Universidad Complutense de Madrid, 457 pp

Bardaji, T., Dabrio, C.J., Goy, J.L., Somoza, L. and Zazo, C. (1990). Pleistocene Fan Deltas in Southeastern Iberian Peninsula: Sedimentary Controls and Sea-Level Changes. *In Coarse-Grained Deltas* (eds A. Colella and D.B. Prior). DOI: https://doi.org/10.1002/9781444303858.ch7

Bardají, T., Silva, P.G., Zazo, C., Goy, J.L. (2010). *Cartografía y memoria del Cuaternario, Geomorfología y Procesoso Activos. Mapa Geológico Nacional, Serie MAGNA, 3ª Serie*. IGME.

Bardají, T., Cabero, A., Lario, J., Zazo, C., Silva, P.G., Goy, J.L., Dabrio, C.J. (2015) Coseismic vs. climatic factors in the record of relative sea level changes: an example from the Last Interglacials in SE Spain. *Quaternary Science Reviews* 113, 60-77. DOI: https://doi.org/10.1016/j.quascirev.2014.10.005.

Batlló, J., Martínez-Solares, J.M., Macià, R., Stich, D., Morales, J., Garrido, L. (2015) The autumn 1919 Torremendo (Jacarilla) earthquake series (SE Spain). *Annals of Geophysics* 58 (3), S0324. DOI: http://dx.doi.org/10.4401/ag-6686

Bellon, H., Bordet, P., Montenat, C. (1983). Chronologie du magmatisme néogène des Cordillères bètiques (Espagne méridionale). *Bulletin de la Société Géologique de France* 7, 205–217.

Bolze, J. and Ott d'Estevou, P. (1986). Processus thermo-mecaniques associes it l'evolution des bassins neogenes des Betiques orientales. *Rap. into IGAL, Paris* 38, 92 p.

Booth-Rea, G., Azañón, J.M., García-Dueñas, V., Augier, R. (2003) Uppermost Tortonian to Quaternary depocentre migration related with segmentation of the strike-slip Palomares Fault Zone, Vera Basin (SE Spain). *Comptes Rendus Geoscience* 335 (9), 751-761. DOI: https://doi.org/10.1016/S1631-0713(03)00121-4

Booth-Rea, G., Azañón, J.M., Azor, A., García-Dueñas, V. (2004) Influence of strike-slip fault segmentation on drainage evolution and topography. A case study: the Palomares Fault Zone (southeastern Betics, Spain). *Journal of Structural Geology* 26 (9), 1615-1632. DOI: https://doi.org/10.1016/j.jsg.2004.01.007

Booth-Rea, G., Silva-Barroso, P.G., Santos-García, J.A. (2008) *Memoria asociada a la Hoja 975 (Puerto Lumbreras) de la 3ª serie del Mapa Geológico Digital de España (1:50.000)*. IGME, Madrid, 240pp.

Booth-Rea, G., Bardají, T., Santos-García, J.A. (2009) *Memoria asociada a la Hoja 997 (Águilas) de la 3ª serie del Mapa Geológico Digital de España (1:50.000)*. IGME, Madrid, 221pp.

Borque, M. J., Sánchez-Alzola, A., Martin-Rojas, I., Alfaro, P., Molina, S., Rosa-Cintas, S., Rodrígez-Caderot, G., de Lacy, C., García-Armenteros, J.A., Avilés, M., Herrera-Olmo, A., García-Tortosa, F.J., Estévez, A., Gil, A. (2019). How much Nubia-Eurasia convergence is accommodated by the NE end of the eastern Betic shear zone (SE Spain)? Constraints from GPS velocities. *Tectonics* 38(5), 1824–1839. DOI: https://doi.org/10.1029/2018TC004970

Bousquet, J.C. (1979) Quaternary strike-slip faults in southeastern Spain. *Tectonophysics* 52 (1-4), 277-286. DOI: https://doi.org/10.1016/0040-1951(79)90232-4

Buforn, E., Bezzeghoud, M., Udías, A., Pro, C. (2004) Seismic Sources on the Iberia-African Plate Boundary and their Tectonic Implications. *Pure and applied geophysics* 161, 623–646. DOI: https://doi.org/10.1007/s00024-003-2466-1

Buontempo, L. and Wuestefeld, A. (2012) Complex fault structure interactions of crustal shear zones revealed by seismic anisotropy: an example in the eastern betic cordillera (Spain). *Terra Nova* 25 (1), 57-54. DOI: https://doi.org/10.1111/ter.12005

CNIG (Centro Nacional de Información Geográfica) Downloads Centre. https://centrodedescargas.cnig.es/CentroDescargas/index.jsp. (Accessed October 2024)

Coppier, G., Griveaud, P., de Larouziere, F-D., Montenat, C., Ott d'Estevou, P. (1989) Example of Neogene tectonic indentation in the Eastern Betic Cordilleras: the Arc of Aguilas (Southeastern Spain). Geodinamica Acta 3 (1), 37-51, DOI: https://doi.org/10.1080/09853111.1989.11105173

Coppier, G., Ott d'Estevou, P., Montenat, C. (1990) Kinematics and paleogeographic evolution of the Eastern Almeria basins. *Documents et travaux de l'IGAL* 12-13, 189-193.

Corbella Marti, J.H. (1969). *Etude géologique de la Sierra de las Moreras (Murcia, Espagne).* Thèse 3ème cycle. University of Paris 6, 158 pp

De Larouziere, F.D., Montenat, C., Ott d'Estevou, P., Griveaud, P. (1987). - Evolution simultanee de bassins neogenes en compression et en extension dans un couloir de decrochement: Hinojar et Mazarron (Sud-Est de l'Espagne). *Bulletin Du Centre De Recherches Elf Exploration Production* 11 (1), 23-38.

De Larouziere, F.D., Bolze, J., Bordet, P., Hernandez, J., Montenat, C., Ott d'Estevou, P. (1988). The Betic segment of the lithospheric Trans-Alboran shear zone during the Late Miocene. *Tectonophysics*, 152, p. 41-52.

De Larouziere, F.D. and Ott d'Estevou, P. (1990) Les Bassins d'Hinojar et de Mazarron. Les Bassins Néogènes du Domaine Betique Oriental (Espagne). *Documents et travaux de l'IGAL* 12-13, 207-220.

DeMets, C., Gordon, R.G., Argus, D.F. (2010) Geologically current plate motions. *Geophysical Journal International* 181 (1), 1–80. DOI: https://doi.org/10.1111/j.1365-246X.2009.04491.x

Díaz del Río, V. (1991) *El margen continental Bético Mediterraneo. Extremo Bético Oriental: Cuenca de Murcia - Escarpe de Mazarron*. Madrid. Publicaciones especiales del Instituto Español de Oceanografía 6, 239 pp.

Duggen, S., Hoernle, K., Van den Bogaard, P., Garbe-Schönberg. D. (2005). Post-Collisional Transition from Subduction- to Intraplate-type Magmatism in the Westernmost Mediterranean: Evidence for Continental-Edge Delamination of Subcontinental Lithosphere. J*ournal of Petrology* 46 (6), 1155–1201. DOI: https://doi.org/10.1093/petrology/egi013

Durand-Delga, M. and Fontboté, J.M. (1980) Le cadre structural de la Méditerranée occidentale. XXVIth Intern. Geological Congress. Colloque C5: Géologie des chaînes alpines issues de la téthys. *Mém. Bur. Rech. Géol. Min., Orléans* 11, 65–85.

Echeverria, A., Khazaradze, G., Asensio, E., Gárate, J., Dávila, J. M., Suriñach, E. (2013). Crustal deformation in eastern Betics from CuaTe-Neo GPS network. *Tectonophysics* 608, 600–612. DOI: https://doi.org/10.1016/j.tecto.2013.08.020

Echeverria, A., Khazaradze, G., Asensio, E., Masana, E. (2015). Geodetic evidence for continuing tectonic activity of the Carboneras fault (SE Spain). *Tectonophysics* 663, 302–309. DOI: https://doi.org/10.1016/j.tecto.2015.08.009

Egeler, C. G. and Simon, O. J. (1969). Orogenic evolution of the Betic Zone (Betic Cordilleras, Spain), with emphasis on the nappe structures. *Geologie en Mijnbouw* 48, 296-305

Fallot, P. (1948). Les Cordillères Bétiques. *Estudios Geológicos* 4, 83-172.

Galindo-Zaldívar, J., González-Lodeiro, F., Jabaloy, A. (1993) Stress and palaeostress in the Betic-Rif cordilleras (Miocene to the present). Tectonophysics 227 (1-4), 105-126. DOI: https://doi.org/10.1016/0040-1951(93)90090-7

García-Dueñas, V., Balanyá, J.C., Martínez Martínez, J.M. (1992) Miocene extensional detachments in the outcropping basement of the northern Alboran basin (Betics) and their implications. *Geo-Marine Letters* 12 (2-3), 88–95. DOI: https://doi.org/10.1007/BF02084917

García-Mayordomo, J. (2005) *Caracterización y análisis de la peligrosidad sísmica en el sureste de España*. PhD Thesis, Universidad Complutense de Madrid. 373 pp.

García-Mayordomo, J., Insua-Arévalo, J.M., Martínez-Díaz, J.J., Jiménez-Díaz, A., Martín-Banda, R., Martín-Alfageme, S., Álvarez-Gómez, J.A., Rodríguez-Peces, M., Pérez-López, R., Rodríguez-Pascua, M.A., Masana, E.,Perea, H., Martín-González, F., Giner-Robles, J., Nemser, E.S., Cabral, J. and the QAFI Compilers Working Group (2012) The Quaternary Faults Database of Iberia (QAFI v.2.0). *Journal of Iberian Geology,* 38(1), 285-302.

García-Mayordomo, J. and R. Martín-Banda (2022) *Guide for the use of QAFI v.4,* In: http://info.igme.es/qafi/ – Instituto Geológico y Minero de España (IGME), CSIC,Madrid, Spain. doi: 10.13140/RG.2.2.12873.01121

García-Tortosa, F.J. (2002) *Los Complejos Tectónicos Alpujárride y Maláguide en el Sector Oriental de la Zona Interna Bética*. PhD Thesis. Universidad de Granada, 413 pp.

García-Tortosa, F. J., López-Garrido, A. C., Sanz de Galdeano, C. (2000). Las unidades de Cabo Tiñoso y Peñas Blancas: revisión y caracterización estratigráfica de las unidades alpujárrides del sector entre Mazarrón y Cartagena (Murcia, España). *Estudios Geológicos* 56(1-2), 31–40. DOI: https://doi.org/10.3989/egeol.00561-2154

García-Tortosa, F.J., Leyva-Cabello, F., Bardají-Azcárate, T. (2004a) Memoria asociada a la *Hoja 976 (Mazarrón) de la 3ª serie del Mapa Geológico Digital de España* (1:50.000). Madrid, IGME. 276 pp.

García-Tortosa, F.J., Leyva-Cabello, F., Cabra-Gil, P. (2004b) Memoria asociada a la *Hoja 977 (Cartagena) de la 3ª serie del Mapa Geológico Digital de España (1:50.000)*. Madrid, IGME. 228 pp.

García-Tortosa, F.J., Leyva-Cabello, F., Cabra-Gil, P. (2004c) Memoria asociada a la *Hoja 978 (Llano del Beal) de la 3ª serie del Mapa Geológico Digital de España (1:50.000)*. Madrid, IGME. 184 pp.

García-Tortosa, F.J., Leyva-Cabello, F., Bardají-Azcárate, T. (2004d) Memoria asociada a la *Hoja 997B (Cope) de la 3ª serie del Mapa Geológico Digital de España (1:50.000).* Madrid, IGME. 117 pp.

Giaconia, F., Booth-Rea, G., Martínez-Martínez, J.M., Azañón, J.M., Storti, F., Artoni, A. (2014) Heterogeneous extension and the role of transfer faults in the development of the southeastern Betic basins (SE Spain). Tectonics 33, 2467–2489. DOI: doi:10.1002/2014TC003681

Gómez de la Peña, L., Ranero, C. R., Gràcia, E., & Booth-Rea, G. (2021). The evolution of the westernmost Mediterranean basins. *Earth-Science Reviews* 214, 103445. DOI: https://doi.org/10.1016/j.earscirev.2020.103445

Gràcia, E., Pallas, R., Soto Juan, I., Comas, M., Moreno, X., Masana, E., Santanach, P., Diez, S., Garcia, M., Danobeitia, J., Bartolome, R., Farran, M., Gomez, M., Alpiste, M.J.R., Lastras, G., Wilmott, V., Perea, H., Blondel, P., Gomez, O., Bullock, L., Jacobs, C., Rouse, I., White, D., Whittle, S., Terrinha, P., Gafeira, J., Roque, C., Hits Scientific Party, I. (2006). Active faulting offshore SE Spain (Alboran Sea); implications for earthquake hazard assessment in the southern Iberian margin. *Earth and Planetary Science Letters* 241 (3–4), 734–749. DOI: http://dx.doi.org/10.1016/j.epsl.2005.11.009

Griveaud, P. (1989) *Etude geologique du secteur d'Aguilas (Sud-Est de l'Espagne): Exemple de poinconnement neogene dans la zone betique interne orientale.* PhD Thesis., University of Lyon I, 198 pp.

Hernandez, J., de Larouziere, F.D., Bolze, J., Bordet, P. (1987) Le magmatisme neogene betico-rifain et le couloir de decrochement trans-Alboran. *Bulletin de la Société Géologique de France* 3 (2), 257–267. DOI: https://doi.org/10.2113/gssgfbull.III.2.257

IGN (Instituto Geográfico Nacional) (n.d.). *Catálogo de terremotos.* https://doi.org/10.7419/162.03.2022

IHM (Instituto Hidrográfico de la Marina) Downloads Centre. https://cdihm.cnig.es/CentroDescargasIHM/home (Accessed 12 September 2025).

ITGE (Instituto Tecnológico Geominero de España) (1990). *Memoria asociada al Mapa Geológico de la Plataforma Continental Española y Zonas Adyacentes (escala 1:200.000), Hoja 79 (Murcia).* ITGE. Madrid. 148 pp.

ITGE-Consejería de Política Territorial y Obras Públicas de la Región de Murcia (1993). *Mapa Neotectónico, Sismotectónico y de Actividad de Fallas de la Región de Murcia a escalas 1:200.000 y 1:100.000.* Memoria. 99 pp

Khazaradze, G., Jacobo-Quiñones, N., Alfaro, P., Medina-Cascales, I., García-Tortosa, F.J., Gil-Cruz, A.J., Rodríguez-Collantes, D., Martin-Rojas, I. (in press) Tectonic salient characterization based on GNSS data: The case of the Eastern Betic Tectonic Arc in the western Mediterranean. *Geodesy and Geodynamics.* DOI: https://doi.org/10.1016/j.geog.2026.06.011

Koulali, A., Ouazar, D., Tahayt, A., King, R.W., Vernant, P., Reilinger, R.E., McClusky, S., Mourabit, T., Davila, J.M., Amraoui, N. (2011) New GPS constraints on active deformation along the Africa–Iberia plate boundary. *Earth and Planetary Science Letters* 308 (1), 211–217. DOI: http://dx.doi.org/10.1016/j.epsl.2011.05.048

Kozur, H., Mulder-Blanken, C., Simón, O.J. (1985). On the Triassic of the Betic Cordilleras (southern Spain), with special emphasis on holothurian sclerites. *Proc. Kon. Ned. Akad. Wetensch* 80, 83-110.

Leyva-Cabello, F., Silva, P.G., García-Tortosa, F.J. (2010) Memoria asociada a la *Hoja 954 (Totana) de la 3ª serie del Mapa Geológico Digital de España* (1:50.000). Madrid, IGME. 224 pp.

Madarieta-Txurruka, A., Prieto, J.F., Escayo, J., Pietrolungo, F., Peláez, J.A., Galindo-Zaldívar, J., Henares, J., Sparacino, F., Ercilla, G., Fernández, J., Palano, M. (2025). New insights on active geodynamics of Iberia and Northwestern Africa from seismic stress and geodetic strain-rate fields. *Gondwana Research* 149, 314-336. DOI: https://doi.org/10.1016/j.gr.2025.08.020

Mandeville, C.R.M. (1993) *A structural study of an arcuate thrust belt, prebetic zone, Southern Spain*. PhD Thesis. University of Oxford. 328 pp. DOI: https://dx.doi.org/10.5287/ora-ngkxvowk5

Manteca-Martínez, J.I., Rodríguez Martínez-Conde, J.A., Puga, E., Díaz de Federico, A. (2004). Deducción de la existencia de un relieve nevado-filábride durante el Mioceno medio–superior, actualmente bajo el mar, al sur de las sierras costeras alpujárrides de El Roldán y La Muela (oeste de Cartagena, Cordillera Bética Oriental). *Revista de la Sociedad Geológica de España* 17 (1-2), 27-37, http://hdl.handle.net/10317/419

Martín-Algarra, A. (1987) *Evolución geológica alpina del contacto entre las Zonas Internas y las Zonas Externas de la (Cordillera Bética).* PhD Thesis, Universidad de Granada. 1271 pp.

Martín-Banda, R., García-Mayordomo, J., Insua-Arévalo, J.M., Salazar, A.E., Rodríguez-Escudero, E., Álvarez-Gómez, J.A., Medialdea, A., Herrero, M.J. (2016) New insights on the seismogenic potential of the Eastern Betic Shear Zone (SE Iberia): Quaternary activity and paleoseismicity of the SW segment of the Carrascoy Fault Zone. *Tectonics* 35, 55–75, DOI: https://doi.org/10.1002/2015TC003997

Martin-Rojas, I., Alfaro, P., Estévez, A. (2015). 3D geometry of growth strata in a fault-propagation fold. Insights into space-time evo-lution of the Crevillente Fault (Abanilla-Alicante

837 sector), Betic Cordillera, Spain. *International Journal of Earth Sciences* 104, 1387–1404. DOI:
838 https://doi.org/10.1007/s00531-015-1143-9

839 Martínez-Díaz, J.J., Masana, E., Ortuño, M. (2012). Active tectonics of the Alhama de Murcia
840 fault, Betic Cordillera, Spain. *Journal of Iberian Geology* 38 (1), 269–286. DOI: http://dx.doi.org/
841 10.5209/rev_JIGE.2012.v38.n1.39218

842 Martínez-Solares, J. M. and Mezcua, J. (2002) *Catálogo sísmico de la Península Ibérica* (880 AC-
843 1900). Monografía nº 18 Instituto Geográfico Nacional, Madrid, Spain, 254 pp.

844 Masana, E., Martínez-Díaz, J.J., Hernández-Enrile, J.L., Santanach, P. (2004) The Alhama de
845 Murcia fault (SE Spain), a seismogenic fault in a diffuse plate boundary: Seismotectonic
846 implications for the Ibero-Magrebian region. *Journal of Geophysical Research* 109, B01301. DOI:
847 https://doi.org/10.1029/2002JB002359

848 Medina-Cascales, I., Martin-Rojas, I., García-Tortosa, F.J., Alfaro, P. (in press) La falla de Terreros
849 (Arco de Águilas, SE de España). Evidencias de actividad cuaternaria. *Geogaceta*

850 Montenat C. (1973) L*es formations neogenes et quaternaires du Levant espagnol (Provinces*
851 *d'Alicante et de Murcie).* PhD Thesis. University of Orsay. 1170 pp.

852 Montenat, C. (1977) Les bassins néogènes du Levant d'Alicante et de Murcia. Stratigraphie,
853 Paltogtographie et Evolution Dynamique. *Documents des laboratoires de géologie de la Faculté*
854 *des Sciences de Lyon* 69, 345 pp.

855 Montenat, C. and Ott d'Estevou (1988) Modalités de structuration synsédimentaire des basins
856 néogènes des Cordillères bètiques orientales». *Résumés communicatios, Symposium "Geology*
857 *of the Pyrenees and the Betics"*, Barcelona, 11-15.

858 Montenat, C. and Ott d'Estevou (1992) Geodynamics of eastern Betic late neogene basins. A
859 review. *Fisica de la Tierra* 4, 57-75.
860 https://dialnet.unirioja.es/servlet/articulo?codigo=124505&orden=1&info=link

861 Montenat, C. and Ott d'Estevou (1999) The diversity of late Neogene sedimentary basins
862 generated by wrench faulting in the eastern Betic Cordillera, SE Spain. *Journal of Petroleum*
863 *Geology* 22, 61-80. DOI: https://doi.org/10.1111/j.1747-5457.1999.tb00459.x

864 Montenat, C. and Serrano, F. (1995) Chapter E8 Potential integrated upper Miocene stratigraphy
865 in southeastern Spain. *Developments in Palaeontology and Stratigraphy* 15, 547-552. DOI:
866 https://doi.org/10.1016/S0920-5446(06)80040-3

867 Montenat, C., Ott d'Estevou, P., Masse, P. (1987). Tectonic-sedimentary characters of the Betic
868 Neogene basins evolving in a crustal transcurrent shear zone (SE Spain). *Bulletin Du Centre De*
869 *Recherches Elf Exploration Production* 11 (1), 1-22.

870 Montenat, C., Ott d'Estevou, P., Coppier, G. (1990) Les bassins neogenes entre Alicante et
871 Cartagena. *Documents et travaux de l'IGAL* 12-13, 313-368.

872 Muñoz D. and Udías A. (1991) *Three large historical earthquakes in Southern Spain*. In: J. Mezcua
873 and A. Udías (eds.), Seismicity, Seismotectonics and Seismic Risk of the Ibero-Maghrebian
874 Region, Monografía n. 8, Instituto Geográfico Nacional, Madrid, 175-182.

875 Nocquet, J. (2012). Present-day kinematics of the Mediterranean: A comprehensive overview of
876 GPS results. *Tectonophysics* 579, 220–242. DOI: https://doi.org/10.1016/j.tecto.2012.03.037

Ortiz, J.E., Torres, T., Sánchez-Palencia, Y., Ros, M., Navarro, F., López-Cilla, I., Galán, L.A., Ramallo, S., Rodríguez Estrella, T., Blázquez, A. (2020) Biomarkers in coastal marshlands: Environmental characteristics of the Mazarrón Basin during the Middle Pleistocene (MIS 7) and Holocene (MIS 1). *Organic Geochemistry* 149, 104117. DOI: https://doi.org/10.1016/j.orggeochem.2020.104117

Ott D'Estevou, P. and Montenat, C. (1985). – Evolution structurale de la zone betique orientale (Espagne) du Tortonien aI'Holocene. *C.R. Acad. Sc. Paris* 300, 363-368.

Ott d'Estevou, P., Montenat, C., Ladure, F., Pierson d'Autrey, L. (1988). - Evolution tectono-sedimentaire du domaine prebetique oriental (Espagne) au Miocene. *C.R. Acad. Sci. Paris* 307, 789-796

Palano, M., González, P. J., Fernández, J. (2015). The Diffuse Plate boundary of Nubia and Iberia in the Western Mediterranean: Crustal deformation evidence for viscous coupling and fragmented lithosphere. *Earth and Planetary Science Letters* 430, 439–447. DOI: https://doi.org/10.1016/j.epsl.2015.08.040

Pérez-Peña, A., Martín-Dávila, J., Gárate, J., Berrocoso, M., Buforn, E. (2010) Velocity field and tectonic strain in Southern Spain and surrounding areas derived from GPS episodic measurements. *Journal of Geodynamics* 49 (3-4), 232-240. DOI: https://doi.org/10.1016/j.jog.2010.01.015

Pérez-Valera, F., Sánchez-Gómez, M., Pérez-López, A., Pérez-Valera, L.A. (2017). An evaporite-bearing accretionary complex in the northernfront of the Betic-Rif orogen. *Tectonics* 36(6): 1006-1036. DOI: https://doi.org/10.1002/2016TC004414

Pérez-Valera, L.A., Villalaín, J.J., Pérez-Valera, F., Azor, A., Sánchez-Gómez, M. (2022). Variably rotated lamproite dikes within a transpressive fault zone: Structural and paleomagnetic analysis of the Socovos Fault zone (Eastern Betics, SE Spain). *Journal of Structural Geology* 165, 104746. DOI: https://doi.org/10.1029/2001TC001321

Platt, J., Allerton, S., Kirker, A., Mandeville, C., Mayfield, A., Platzman, E.S., Rimi, A. (2003). The ultimate arc: Differential displacement, oroclinal bending, and vertical axis rotation in the External Betic-Rif arc. *Tectonics* 22(3), 1017. doi:10.1029/2001TC001321

Portela, J., Staller, A., Béjar-Pizarro, M., Martínez-Díaz, J.J., Álvarez-Gómez, J.A., Khazaradze, G. (2025) New Insights on the Crustal Deformation in the Eastern Betics from Densified GNSS Data. Tectonics 44 (2), e2024TC008381. DOI: https://doi.org/10.1029/2024TC008381

Puga, E., Díaz de Federico, A., Fontboté, J.M. (1974). Sobre la individualización y sistematización de las unidades profundas de la Zona Bética. *Estudios Geológicos* 30, 543-548.

Rodrigo-Naharro, J.; Aracil, E.; Perez del Villar, L. (2013) *Geophysical Research in the Ganuelas-Mazarron Tertiary Basin (Murcia, Spain), as a Natural Analogue of CO {sub 2} Storage and Leakage.*

Rodrigo-Naharro, J., Aracil, E., Pérez del Villar, L. (2018). Geophysical investigations in the Gañuelas-Mazarrón Tertiary basin (SE Spain): a natural analogue of a geological CO2 storage affected by anthropogenic leakages. *Journal of Applied Geophysics* 155, 187–198. DOI: https://doi.org/10.1016/j.jappgeo.2018.06.006

Rodríguez-Estrella, T. (1979). *Geología e Hidrogeología del sector de Alcaraz-Lietor-Yeste* (Albacete). IGME. 276 pp.

Sanz de Galdeano, C. (1983) Los accidentes y fracturas principales de las Cordilleras Béticas. *Estudios Geológicos* 39, 157-165.

Sanz de Galdeano, C. (1990) Geologic evolution of the Betic Cordilleras in the Western Mediterranean, Miocene to the present. *Tectonophysics* 172 (1-2), 107-119. DOI: https://doi.org/10.1016/0040-1951(90)90062-D

Sanz de Galdeano, C. (1997) *La Zona Interna Bético-Rifeña*. Monográficas del Sur. Universidad de Granada, 316 pp. ISBN: 84-338-2312-4

Serpelloni, E., Vannuci, G., Pondrelli, S., Argnani, A., Casula, G., Anzidei, M., Baldi, P., Gasperini, P. (2007) Kinematics of the Western Africa-Eurasia plate boundary from focal mechanisms and GPS data. *Geophysical Journal International* 169 (3), 1180-1200. DOI: https://doi.org/10.1111/j.1365-246X.2007.03367.x

Silva, P.G., Goy, J.L., Somoza, L., Zazo, C., Bardají, T. (1993) Landscape response to strike-slip faulting linked to collisional settings: Quaternary tectonics and basin formation in the Eastern Betics, southeastern Spain. *Tectonophysics* 224 (4), 289-303. DOI: https://doi.org/10.1016/0040-1951(93)90034-H

Spakman, W., Chertova, M.V., van den Berg, A., van Hinsbergen, D.J.J. (2018) Puzzling features of western Mediterranean tectonics explained by slab dragging. *Nature geoscience* 11, 211-216. DOI: https://doi.org/10.1038/s41561-018-0066-z

Stich, D., Serpelloni, E., de Lis Mancilla, F., Morales, J. (2006). Kinematics of the Iberia–Maghreb plate contact from seismic moment tensors and GPS observations. *Tectonophysics* 426(3), 295-317. https://doi.org/10.1016/j.tecto.2006.08.004

Tapponnier, P., 1977. Evolution tectonique du systtme alpin en Mediterranee: poinconnement et Ccrasement rigide-plastique. *Bulletin de la Société Géologique de France* 7, 437-460.

Trigueros-Ramos, L., Sánchez-Gómez, M., Pérez-Valera, L.A., Sanz, D., Pérez-Valera, F. (2024) La estructura frontal del arco de Cazorla-Alcaraz en el sector de Vianos (Prebético Externo, SE España). *Geogaceta* 76, 39-42. DOI: https://doi.org/10.55407/geogaceta104518

Torres, T., Ortiz, J.E., Sánchez-Palencia, Y., Ros, M., Navarro, F., López-Cilla, I., Galán, L.A., Ramallo, S., Rodríguez-Estrella, T., Blázquez, A. (2020) The Pleistocene and Holocene records of the Mazarrón Basin (SE Spain). *Quaternary International* 566–567, 256-270. DOI: https://doi.org/10.1016/j.quaint.2020.03.019.

Vernant, P., Fadil, A., Mourabit, T., Ouazar, D., Koulali, A., Davila, J.M., Garate, J., McClusky, S., Reilinger, R. (2010) Geodetic constraints on active tectonics of the Western Mediterranean: implications for the kinematics and dynamics of the Nubia–Eurasia plate boundary zone. *Journal of Geodynamics* 49 (3), 123–129. DOI: http://dx.doi.org/10.1016/j.jog.2009.10.007.

Zazo, C., Goy, J.L., Dabrio, C.J., Bardají, T., Hillaire-Marcel, C., Ghaleb, B., González-Delgado, J.A., Soler, V. (2003) Pleistocene raised marine terraces of the Spanish Mediterranean and Atlantic coasts: records of coastal uplift, sea-level highstands and climate changes. *Marine Geology* 194